

<b>Antragstyp</b>	Schwerpunktprogramm - Einzelantrag - Neuantrag
<b>Type of Proposal</b>	Priority Programme - Individual Proposal - New Proposal
<b>Antragsdauer / Requested Duration</b>	36 Monate / 36 months
<b>Fach</b>	Theoretische Physik der kondensierten Materie
<b>Subject Area</b>	Theoretical Condensed Matter Physics
<b>Rahmenprojekt / Framework Project</b>	SPP 2171
<b>Titel</b>	<b>Mathematische Modellierung und Simulation der Wechselwirkung von Substraten mit Strömungen durch verallgemeinerte Gradientenflüsse</b>
<b>Title</b>	<b>Mathematical modeling and simulation of substrate-flow interaction using generalized gradient flows</b>
<b>Geschäftszeichen / Reference No.</b>	<b>PE 1782/2-1</b>
<b>Antragsteller / Applicant</b>	<b>Dr. Dirk Peschka</b> Weierstraß-Institut für Angewandte Analysis und Stochastik (WIAS) Forschungsgruppe Modellierung, Analysis u Skalenübergänge von Volumen-Grenzschicht-Prozessen Berlin
<b>Arbeitgeberzusage / Statement by Employer</b>	Die Erklärung zur Arbeitgeberfunktion liegt noch nicht vor. A statement regarding employer status has not yet been received.

**Beantragte Mittel / Budget Request:**

	<b>Beantragt / Requested</b>		
<b>Dauer [Monate] / Duration [Months]</b>	<b>36</b>		
<b>PE 1782/2-1</b>			
<b>Summe / Total [Euro]</b>	<b>225.450</b>		
<b>Dr. Dirk Peschka</b>			
	<b>Anz. / No.</b>	<b>Dauer / Duration</b>	<b>Euro</b>
<b>Personalmittel / Funding for Staff</b>			<b>209.700</b>
Eigene Stelle 100 % / Temporary Position for Principal Investigator 100 %	1	36	209.700
<b>Sachmittel / Direct Project Costs</b>			<b>15.750</b>
Gäste / Visiting Researchers			4.500
Publikationen / Publications			2.250

Reisen / Travel				9.000
-----------------	--	--	--	-------

**Zusammenfassung** Der Antrag im Schwerpunktprogramm „Dynamic Wetting of Flexible, Adaptive and Switchable Surfaces“ (SPP 2171) befasst sich mit der thermodynamisch konsistenten Behandlung von Strömungen auf Substraten, deren Dynamik stark an die Eigenschaften bzw. die Dynamik dieses Substrates gekoppelt ist. Methodisch konzentriert sich die Arbeit dabei auf sogenannte Gradientenflüsse, d.h. Modellbeschreibungen bei denen konservative Kräfte im optimalen Gleichgewicht mit dissipativen Reibungskräften stehen. Während solche Beschreibungen im klassischen Fall von quadratischer Dissipation im Volumen bereits relativ gut untersucht sind, ist das Ziel des vorliegenden Antrages die systematische Erweiterung dieser Ansätze auf nicht-quadratische Dissipation unter der Einbeziehung von Grenzflächen und Kontaktlinien. Insbesondere für Entnetzungsprozesse haben die Vorarbeiten des Antragstellers klar gezeigt, dass die Einbeziehung solcher Ansätze von essentieller Bedeutung für physikalisch realistische Beschreibungen ist.

In der theoretischen Beschreibung geht es hierbei vor allen Dingen um Kontinuumsmodelle mit scharfen Grenzflächen und bewegten Kontaktlinien, wobei hier sowohl (Navier)-Stokes Gleichungen als auch reduzierte Modelle für dünne Filme betrachtet werden sollen. Neben der Entwicklung von Modellstrukturen ist die Implementation entsprechender numerischer Verfahren auf Basis von finiten Elementen ein integraler Bestandteil dieses Antrages. Hier stehen besonders die Fragestellungen der numerischen Behandlung von verallgemeinerten Gradientenstrukturen mit Hysterese und die Bewegung von Gebieten mit sogenannten „Arbitrary Lagrangian Eulerian“ Verfahren im Vordergrund.

Die entwickelten Methoden sollen dann auf unterschiedlichen Anwendungsszenarien anderer Projekte des Schwerpunktprogramms übertragen werden: Naheliegend ist der Vergleich der numerischen Methoden mit unterschiedlichen numerischen Verfahren anderer Kollegen. Weiterhin erlaubt die energetische Formulierung die Beschreibung chemisch heterogener Substrate (z.B. energetischer Stufen), mit denen z.B. die Entnetzungsdynamik von Tropfen direkt beeinflusst werden kann. Die konkrete Entwicklung der Volumen/Grenzflächen/Kontaktlinien-Kopplung ist in Zusammenarbeit mit anderen Projekten geplant. Die Kopplung an Substrate mit einer eigenen Dynamik soll für poröse Substrate, Substrate mit „Surfactants“ und deformierbare Substrate erfolgen.

**Summary** The proposal in the priority program "Dynamic Wetting of Flexible, Adaptive and Switchable Surfaces" (SPP 2171) considers the thermodynamically consistent treatment of flows over substrates whose dynamics is strongly coupled to the properties or the dynamics of this substrate. Methodically, the work concentrates on so-called gradient flows, i.e. model descriptions in which conservative forces are in optimal equilibrium with dissipative friction forces. While such descriptions are already well studied in the classical case, i.e. quadratic dissipation in volume, the aim of the present proposal is the systematic extension of these approaches to non-quadratic dissipation and the inclusion of free interfaces and contact lines. Especially for dewetting processes, the preliminary work of the applicant has clearly shown that the inclusion of such approaches is of essential importance for physically realistic .

The theoretical description is mainly concerned with continuum models with sharp interfaces and moving contact lines, where both (Navier)-Stokes equations and reduced models for thin films will be considered. In addition to the development of model structures, the implementation of numerical methods based on finite elements is an integral part of this proposal. In particular, the numerical treatment of generalized gradient structures with

hysteresis and the movement of regions with so-called Arbitrary Lagrangian Eulerian methods are the main topics.

The developed methods will then be transferred to different applications of other projects in the priority program: Numerical methods will be compared with different approaches of other colleagues. Furthermore, the energetic formulation allows the description of chemically heterogeneous substrates (e.g. energetic steps), with which, e.g., the dewetting dynamics of droplets can be directly influenced. The concrete development of the volume/interface/contact line coupling is planned in cooperation with other projects. The coupling to substrates with their own dynamics will take place for porous substrates, substrates with "surfactants" and deformable substrates.

**Project Description – Project Proposal: Dr. Dirk Peschka, Weierstrass Institute, Berlin**

# Mathematical modeling and simulation of substrate-flow interaction using generalized gradient flows

---

## Project Description

### 1 State of the art and preliminary work

When considering bulk fluid flow, the main source of energy dissipation that is usually considered is the fluids *viscosity*. As soon as one takes into account the interaction of the fluid with a substrate, one needs to consider further mechanisms of *energy dissipation*: The generally accepted (linear) boundary condition at the fluid-substrate interface is the *Navier-slip* condition

$$\mathbf{t} \cdot \boldsymbol{\tau} \mathbf{n} = -\mu_\Gamma \mathbf{u} \cdot \mathbf{t}. \quad (1)$$

It states that shear-stress  $\mathbf{t} \cdot \boldsymbol{\tau} \mathbf{n}$  and slip-velocity  $\mathbf{u} \cdot \mathbf{t}$  at the interface are proportional and thereby effectively assigns a certain amount of dissipation  $\frac{1}{2}\mu_\Gamma|\mathbf{u} \cdot \mathbf{t}|^2$  to that interface. Sending the corresponding friction coefficient  $\mu_\Gamma$  to infinity lets one recover the classical *no-slip* boundary condition, whereas for vanishing friction coefficient one recovers a *no-shear-stress* boundary condition. Additionally considering moving contact lines with no-slip condition, the impact of microscopic properties, e.g., surface roughness or chemical heterogeneities, on the dynamics at macroscopic scales becomes apparent but its description is complicated due to the appearance of singular stresses at the contact line. While the Navier-slip condition makes this singularity integrable, adding further *contact line dissipation* allows it to introduce models for *dynamic contact angles*. Obviously, the phenomena observed in reality, e.g., pattern formation, time-scales etc., can be drastically different depending on the magnitude of each of these contributions to the dissipation.

Taking into account additional physics in the substrate or on the interface can give these energetic contributions a concrete interpretation: *soft substrates* deform and have dissipation on their own; *surfactants* can move from bulk/surface (soluble/insoluble) liquid to the substrate and modify the surface energy; liquids can diffuse/flow into *porous substrates* and modify interface dissipation. In all of the above cases there is an intricate nonlinear interaction of flow and substrate physics. However, even without such a nonlinear coupling, the control of global and local surface energy and dissipation properties can be used to *control the flow* in a desired direction or to produce certain desired *dewetting patterns*. Hence, this motivates the goal of this proposal:

**Goal:** *The development of thermodynamically consistent models and numerical schemes for substrate-flow coupling and for control of flow based on energy-dissipation formulations for bulk, interfaces, and the contact line of the multiphysics system. The primary focus will be the embedding of dynamic contact angles into settings with strong substrate-flow coupling.*

The goal of the Priority Programme 2171 is to obtain a fundamental and deep understanding of the dewetting & wetting of flexible, adaptive and switchable substrates from an experimental and theoretical point-of-view. As this shall be restricted to simple liquids, this implies a simple relationship of stress  $\boldsymbol{\tau}$  and velocity  $\mathbf{u}$ , i.e.,  $\boldsymbol{\tau} = \boldsymbol{\tau}(\mathbb{D}\mathbf{u})$  where  $\mathbb{D}\mathbf{u} = \frac{1}{2}(\nabla \mathbf{u} + \nabla \mathbf{u}^\top)$ . However, even for simple fluids the partial differential equations (PDE) for dewetting are highly nonlinear due to the fact that the Navier-Stokes problem is coupled to the motion of a time-dependent domain and thereby becomes a *free boundary problem*. Treating such a physical problem alone presents a couple of mathematical challenges. Furthermore, the strong coupling to substrate

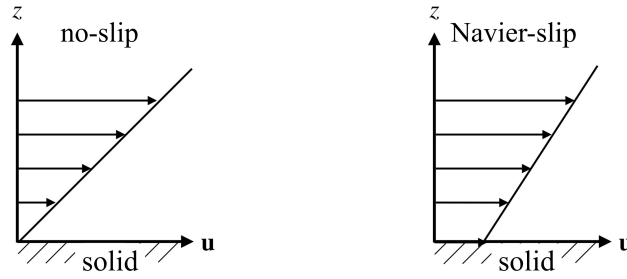


**Figure 1:** Sketch of near-substrate flow profile (**left**) with no-slip and (**right**) Navier-slip.

dynamics requires a systematic method to introduce physical and mathematical feasible coupling mechanisms, *i.e.*, in the sense of *Onsager reciprocity* or *thermodynamic consistency* [1, 2, 3].

**Navier-Stokes Free Boundary Problem with Contact Lines:** For incompressible Newtonian fluids with viscosity  $\mu > 0$  the relation of velocity  $\mathbf{u}(t, \mathbf{x}) \in \mathbb{R}^d$  at time  $t$  in the domain  $\Omega(t) \subset \mathbb{R}^d$  and the stress tensor  $\boldsymbol{\tau}(\mathbf{u}) : \Omega \rightarrow \mathbb{R}^{d \times d}$  is given by

$$\boldsymbol{\tau}(\mathbf{u}) = 2\mu \mathbb{D}\mathbf{u}. \quad (2)$$

While  $\boldsymbol{\tau}(\mathbf{u})$  is the prototype tensor for bulk effects of simple viscous flows, the no-slip condition

$$\mathbf{u} = \mathbf{0} \quad \text{on} \quad \Gamma(t), \quad (3)$$

is assumed to be the prototype boundary condition at solid-fluid interfaces  $\Gamma$ . Balance of momentum and mass then lead to the Navier-Stokes equation in a time-dependent domain  $\Omega(t)$

$$\partial_t(\rho\mathbf{u}) + \mathbf{u} \cdot \nabla(\rho\mathbf{u}) = -\nabla p + \operatorname{div} \boldsymbol{\tau}(\mathbf{u}) + \mathbf{f}, \quad \nabla \cdot \mathbf{u} = 0, \quad (4)$$

where we seek the velocity  $\mathbf{u}(t, \cdot) : \Omega(t) \rightarrow \mathbb{R}^d$  and the pressure  $p(t, \cdot) : \Omega(t) \rightarrow \mathbb{R}$ . This partial differential equation is coupled with appropriate conditions at boundaries, interfaces, contact lines and provided with initial data  $\mathbf{u}(t = 0, \cdot) = \bar{\mathbf{u}}$  and  $\Omega(t = 0) = \bar{\Omega}$ . The domain  $\Omega(t)$  evolves according to a *kinematic condition*, which makes this PDE problem a free boundary problem. In a microfluidic setting the no-slip boundary condition (3) is often replaced by the Navier-slip condition in (1), where the friction coefficient  $\mu_\Gamma := \mu/b > 0$  is associated with the well-known *slip length*  $b$ , see also Fig. 1. In particular, for flows near a moving contact line  $\partial\Gamma(t)$ , the Navier-slip condition offers one out of various possible mechanism to remove the non-integrable stress singularity at a sliding contact line [4]. Influenced by physical and chemical interface properties such as hydrophobicity, surface roughness, coating or viscoelastic properties, different measuring techniques have found slip-lengths ranging from a few nanometers up to several micrometers, also indirectly visible by its impact on pattern formation processes. The validity of slip in microfluidic settings is undisputed nowadays [5]. Thin-film models with different magnitudes of dissipation  $\mu_\Gamma$  have been investigated in [6] and were extended to multiphase flows in [P1].

Free boundary problems become more complex when considering moving contact lines. Interfacial tensions between solid-vapor  $\gamma_{SV}$ , solid-liquid  $\gamma_{SL}$  and liquid-vapor  $\gamma$  lead to equilibrium contact angles  $\vartheta = \vartheta_e$  determined by the famous Young-Dupré equation

$$\gamma(\cos(\vartheta_e) - 1) = S \quad \text{at} \quad \partial\Gamma(t), \quad (5)$$

with spreading coefficient  $S = \gamma_{SV} - (\gamma_{SL} + \gamma)$  on rigid substrates or by the Neumann triangle construction when considering soft elastic or liquid substrates. The physics becomes even more

involved for contact lines moving over *physically realistic nonideal surfaces*, e.g., which are not perfectly smooth, rigid or chemically homogeneous. While molecular kinetic models are useful to understand the microscopic origins of contact line motion, this proposal employs hydrodynamic descriptions with sharp interfaces. Primarily for liquid-liquid-solid junctions rolling motion was observed and thermodynamic descriptions have been developed, e.g., [7, 8], but the focus here is on sliding motion and stick-slip. For sliding contact lines, models with contact angle hysteresis/stick-slip and empirical laws for contact line dynamics are discussed in the literature, e.g., see [9, 10]. In the Young-Dupré equation (5) the spreading coefficient needs to be replaced using the Cassie-Baxter relation with the homogenized coefficient  $\bar{S}$  [11].

However, the corresponding equilibrium angle might never be attained. Due to pinning at microscopic defects, the contact line is stationary for contact angles  $\vartheta_r < \vartheta < \vartheta_a$  and only starts to advance or recede beyond these values. Models for smooth contact line dynamics without hysteresis are often based on empirical laws and microscopic theories. For instance, assuming an energy-dissipation balance truncated at a microscopic length scale  $\ell$  and with a macroscopic length scale  $L$  away from the contact line, the theory by Cox and Voinov predicts  $\vartheta^3 - \vartheta_e^3 = \pm 9 \text{Ca} \ln(L/\ell)$ , where the Capillary number  $\text{Ca} = \mu U / \gamma$  depends on dynamic viscosity  $\mu$ , surface tension  $\gamma$  and contact line velocity  $U$  [12]. Another contact line model by Ruschak and Hayes produces a similar law, which, however, was derived from a molecular-kinetic model of wetting using dissipation at the contact line [13]. Most models considered in the literature are of the form  $W(\vartheta, \vartheta_e) = \pm \text{Ca}$  with power-law dependence on angles and  $W(\vartheta_e, \vartheta_e) = 0$ . Using such a dynamic contact angle, one can make predictions for dewetting rates of complex systems, e.g., liquid dewetting, droplet spreading or gravity-driven droplet motion. On the continuum level, an energetic approach to such phenomena can be achieved using variational structures, e.g., see [14], where the corresponding contact line model is

$$\gamma(\cos \vartheta_e - \cos \vartheta) = \mu_\gamma \boldsymbol{\nu}_x \cdot \mathbf{u}_x. \quad (6)$$

**Thermodynamics, Gradient Flows, and the Role of Dissipation:** Nowadays, variational principles are widely used to model complex physical systems with partial differential equations derived from purely energetic arguments, see e.g. [15, 3]. General variational approaches for complex fluids often rely on a classification of dissipative or nondissipative kinematics, e.g., see [16, 17, 18]. For wetting and dewetting flows flows on rigid substrates such formulations have amplified the physical and mathematical understanding of the corresponding free boundary problems [19]. The GENERIC<sup>1</sup> framework of reversible and irreversible processes proposed by Öttinger and Grmela [17] is an advanced variational structure that has been used extensively to model complex fluids, e.g., nonlinear viscoelastic polymers. This construction has been formalized to model a number of thermodynamical processes with convection and diffusion, e.g., [20] and [P2] and transferred to simulations, e.g., see [21].

To define a gradient flow, let  $q \in Q$  be a generalized state with velocities  $\dot{q} \in V$ . Then its evolution, driven by a thermodynamic potential  $\mathcal{E} : Q \rightarrow \mathbb{R}$  such as the free energy, is given by

$$\dot{q}(t) = -\nabla_g \mathcal{E}(q(t)), \quad (7a)$$

where the gradient with respect to the positive symmetric bilinear form  $g_q : V \times V \rightarrow \mathbb{R}$  is defined  $g_q(\nabla_g \mathcal{E}(q), v) = \langle D\mathcal{E}(q), v \rangle$  for all  $v \in V$  and functional derivative  $D\mathcal{E}(q) \in V^*$ . The decay of the (free) energy  $\frac{d}{dt} \mathcal{E}(q(t)) \equiv \langle D\mathcal{E}(q), \dot{q} \rangle = -g_q(\dot{q}, \dot{q}) \leq 0$  holds by construction using (7a).

---

<sup>1</sup>an acronym for General Equations for Non-Equilibrium Reversible Ireversible Coupling

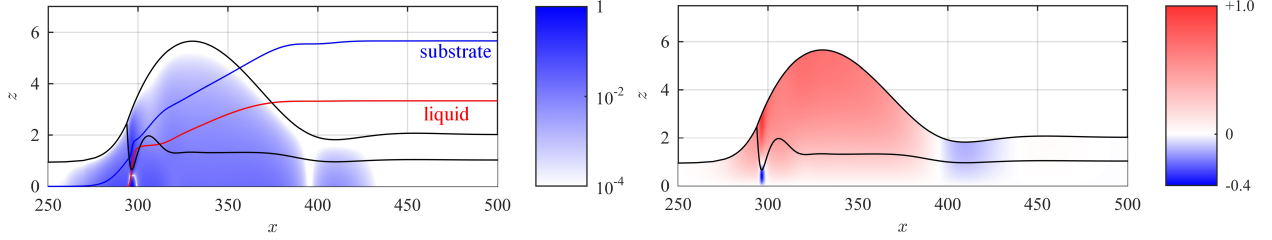


**Figure 2:** Dewetting from soft substrate [P4] (**left**) log-scale local dissipation and (**right**) corresponding local velocity.

Defining  $\mathcal{D}(v) = g_q(v, v)$  we can state an evolution equation that is formally equivalent to (7a):

$$\dot{q} = \operatorname{argmin}_{v \in V} \left( \frac{1}{2} \mathcal{D}(v) + \langle D\mathcal{E}, v \rangle \right). \quad (7b)$$

In the context of fluid flows, this is the Helmholtz-Rayleigh dissipation principle for the dissipation functional  $\mathcal{D} : V \rightarrow \mathbb{R}$  where the velocity corresponds to the flow field  $\dot{q} \simeq \mathbf{u}$  and correspondingly  $v \simeq \mathbf{v}$ . For Newtonian fluids the bulk dissipation is  $\mathcal{D}_{\text{bulk}}(\mathbf{v}) = \int_{\Omega} 2\mu \mathbb{D}\mathbf{v} : \mathbb{D}\mathbf{v} \, dx$  and in [P3] it was demonstrated that a formal gradient structure can be established based on a further decomposition of the total dissipation into contributions  $\mathcal{D} = \mathcal{D}_{\text{bulk}} + \mathcal{D}_{\text{bound}} + \mathcal{D}_{\text{cl}}$ , where

$$\mathcal{D}_{\text{bound}} = \int_{\Gamma \subset \partial\Omega} W_{\text{bound}}(\mathbf{u}) \, da, \quad \mathcal{D}_{\text{cl}} = \int_{\partial\Gamma} W_{\text{cl}}(\mathbf{u}) \, d\ell, \quad (8)$$

and allows it to designate some of the effective substrate-flow interaction into dissipative mechanism. Modeling of dissipation has been extensively discussed for the Navier-slip condition [5] encoded in the boundary term  $W_{\text{bound}}$ , but a detailed study of contact line dynamics based on the dissipation  $W_{\text{cl}}$  is still elusive.

**Coupling Flow via Interfaces with Substrates:** However, variational approaches are also highly useful when considering strongly and nonlinear coupled PDE problem. In a previous study on dewetting from liquid substrates, we showed that explicitly considering the substrate dissipation produces a much deeper understanding of the underlying physical mechanisms [P4], see also Fig. 2. These results were based on an earlier work [P5], where we showed that the gradient flow structure is even useful for the design of complex coupled numerical algorithms with moving contact lines. In this work we developed a gradient flow based algorithm for a thin-film flow dewetting from soft (liquid) substrate [P5], *i.e.*,

$$\partial_t \begin{pmatrix} h_\ell \\ h_s \end{pmatrix} - \nabla \cdot \mathbb{M} \nabla \begin{pmatrix} \pi_\ell \\ \pi_s \end{pmatrix} = 0, \quad \text{wetted area } \omega, \quad (9)$$

$$\partial_t h_s - \nabla \cdot m \nabla \pi_s = 0, \quad \text{dewetted area } \mathbb{R}^{d-1} \setminus \omega, \quad (10)$$

where  $h_s$  encodes the substrate film thickness,  $h_\ell$  is the liquid film thickness as shown in the black lines in Fig. 2, and  $\pi_i$  are the generalized pressures. The main challenge was the construction of a monolithic time-discretization, which features a force balance (Neumann triangle) at the moving contact line  $\partial\omega$  enforced and a corresponding ALE scheme. The corresponding Stokes flow is based on the dissipation

$$\mathcal{D}(\mathbf{u}_s, \mathbf{u}_\ell) = \int_{\Omega_s} 2\mu_s |\mathbb{D}\mathbf{u}_s|^2 \, dx + \int_{\Omega_\ell} 2\mu_\ell |\mathbb{D}\mathbf{u}_\ell|^2 \, dx + \int_{\Gamma} \mu_\Gamma |\mathbf{u}_s - \mathbf{u}_\ell|^2 \, da, \quad (11)$$

and a corresponding solution for  $\mu_\Gamma \rightarrow \infty$  is shown in Fig. 4. Both, Stokes and thin-film are solved

using a finite-element method (FEM) and required the construction of discrete spaces with discontinuous solutions at interfaces/contact lines. Considering the quantitative agreement obtained in [22] and [P4] the thin-film model delivers a prediction in terms of a more efficient/reduced problem formulation. In [P1] we also showed that with finite  $\mu_\Gamma$  corresponding Navier-slip conditions in a multilayer setup can be systematically enforced and a mathematical analysis of stationary solutions was performed in [P6]. In a recent work [23] on multiphase flows (dense suspensions) we worked on the dissipation modeling for suspension flows based on a flow-map concept. This concept is particularly important for complex liquids, but can be easily extended to the problems studied in the Priority Programme: While the fluid behavior is simple and  $W_{\text{bulk}}$  is basically Newtonian, the substrate interaction should be rather complex, possibly leading to complicated interaction mechanisms encoded in boundary and contact line dissipation.

**Numerical Methods for Free Boundary Problems with Contact Lines:** Fluid flows with moving domains are modeled either using diffuse or sharp interface representations. This proposal will focus on the latter and use interface-tracking and ALE methods<sup>2</sup> with conforming finite-elements. This approach has the advantage that it allows a finer control over solutions near contact lines and near interfaces but is problematic for handling topological transitions. For diffuse interface models, on the other hand, topological transitions are unproblematic [24] but require spatial adaptivity to ensure the correct behavior for vanishing layer width.

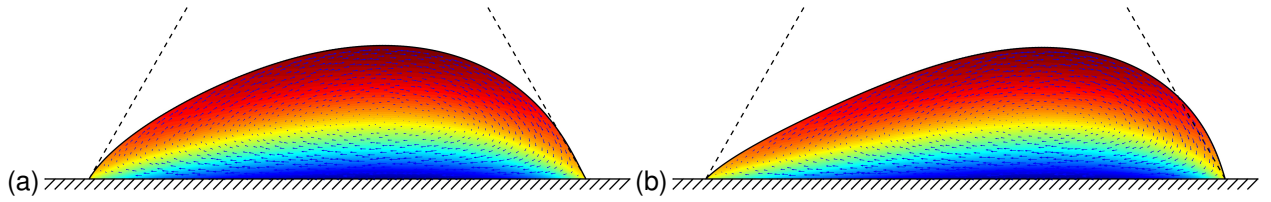


**Figure 3:** Numerical solution of Stokes flow for 2D sliding droplet with gravity in  $+x$  direction (a) with equilibrium angle  $\vartheta = \vartheta_e$  indicated by dashed lines and (b) with smooth dynamic contact angle as in (6) and flow field (arrows  $\sim \mathbf{u}(t, \mathbf{x}) - \bar{\mathbf{u}}$  in comoving frame; shading  $\sim \mathbf{u}(t, \mathbf{x})$  in Eulerian frame) with advancing and receding contact angle.

We will couple ALE methods to gradient flow based models, where the fluid dynamics is strongly coupled to the substrate. Therefore, the main ingredient is a flow map  $\mathbf{X}_t : \bar{\Omega} \rightarrow \mathbb{R}^d$  mapping the reference domain  $\bar{\Omega} = \Omega(t=0)$  to its later state  $\Omega(t) \subset \mathbb{R}^d$ . The corresponding flow field is  $\mathbf{u} = (\partial_t \mathbf{X}_t) \circ \mathbf{X}_t^{-1}$ . Numerical algorithms for fluid flow with moving domains usually solve for  $\mathbf{X}_t$ , where a single step of the time-discretization with flow maps is solved in a spatially fixed frame and one can linearize  $\mathbf{X}_{t_0 \rightarrow t_0 + \Delta t}(\mathbf{x}) = \mathbf{X}_{t_0 + \Delta t} \circ \mathbf{X}_{t_0}^{-1}(\mathbf{x}) \approx \mathbf{x} + (\Delta t)\mathbf{u}(t_0, \mathbf{x})$ . In the literature also higher-order ALE schemes are discussed, e.g. [25]. The spatial discretization of the Stokes free boundary problem for an incompressible fluid uses inf-sup stable isoparametric mixed finite-element pairs, most commonly  $P_2/P_1$  or  $P_2^{\text{bubble}}/P_1^{\text{disc}}$  [26]. The weak formulation of the Stokes problem is a saddle-point problem of the form: Find  $(\mathbf{u}, p) \in (H_0^1(\Omega))^d \times L^2(\Omega) = W$  such that  $a(\mathbf{u}, \mathbf{v}) + (-\nabla p, \mathbf{v})_{L^2} + (q, \nabla \cdot \mathbf{u})_{L^2} = f(\mathbf{v})$  for all  $(\mathbf{v}, q) \in W$ . If the flow is driven by surface energy  $\mathcal{E}_{\text{surf}} = \gamma |\Gamma_f|$ , then we get  $f(\mathbf{v}) = \langle -D\mathcal{E}_{\text{surf}}, \mathbf{v} \rangle$  and obtain the weak form [P3]

$$a(\mathbf{u}, \mathbf{v}) = \int_{\Omega} 2\mu \mathbb{D}\mathbf{u} : \mathbb{D}\mathbf{v} \, dx, \quad f(\mathbf{v}) = - \int_{\Gamma_f} \gamma \operatorname{div}_{\Gamma}(\mathbf{v}) \, da = \int_{\Gamma_f} \gamma \kappa \nu \cdot \mathbf{v} \, da. \quad (12)$$

This indicates how the weak formulation of the problem, including boundary and interface conditions, naturally emerge from energy functionals. Typical numerical issues which arise in such an ALE framework are that the time-discretization suggests a (semi)implicit treatment of the cur-

<sup>2</sup>Acronym for Arbitrary Lagrangian Eulerian referring to methods, where the frame of reference is between Lagrangian (material) and Eulerian (current) point-of-view.

vature, that higher regularity requires to unravel the dependence of dissipation  $\mathcal{D}$  and energy  $\mathcal{E}$  on the state  $\mathbf{X}_t$ , that moving the triangulation according to  $T_k(t) = \mathbf{X}_t(T_k(0))$  has an impact on mesh quality, and that one should avoid spurious velocities. For multiphase flows a common strategy is to enrich the  $L^2$  pressure space approximated by  $P_1$  finite-element functions with an element-wise discontinuous part in  $P_1^{\text{disc}}$ , that is able to absorb the pressure-jump as shown in Fig. 4. For the simulation of bilayer dewetting a related methodology was also used in [P7]. The resulting speed of convergence depends on both the choice of the FE space and on the resolution of the interface.

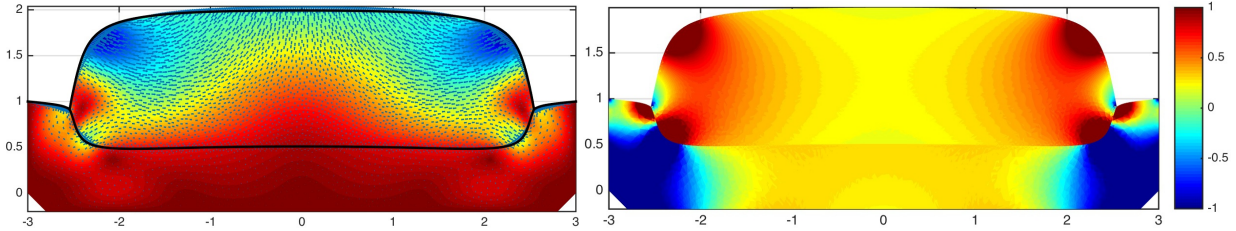


**Figure 4:** Droplet for  $\Omega(t) \subset \mathbb{R}^2$  on a liquid substrate showing (**left**) direction and magnitude of the flow field  $\mathbf{u}$  and the free interfaces and (**right**) the discontinuous pressure with resolved jumps across internal interfaces.

Another problem of ALE methods is caused by the moving mesh, which can become anisotropic or corrupted or develop mathematical & numerical singularities when approaching a topological transition, e.g., corresponding to merging and splitting droplets during film rupture or pinch-off. This is usually addressed using spatial and temporal adaptivity and sophisticated ALE methods to improve the mesh motion [27]. A similar ALE strategy was also used in the  $d = 3$  thin-film setting in [P8] to maintain mesh quality for a longer time, e.g., see Fig. 5.

Thin-film models are reduced models that are easier to analyze and solve. Often, they give qualitative explanation for physical mechanisms [O1] or even quantitative predictions [P4]. Assume the time-dependent domain  $\Omega(t) = \{\mathbf{x} \equiv (x, z) \in \mathbb{R}^{d-1} \times \mathbb{R}_{\geq 0} : 0 < z < h(t, x)\} \subset \mathbb{R}^d$  is parametrized using  $h(t, x) \geq 0$  and  $|\nabla h| \ll 1$ , then the Stokes equation on a planar solid surface can be reduced [28] to a thin-film type equation of the form

$$\partial_t h - \nabla_x \cdot (m(h) \nabla_x \pi) = 0, \quad \pi = \frac{\delta}{\delta h} \mathcal{E}(h), \quad \mathcal{E}(h) = \int_{\mathbb{R}^{d-1}} \frac{1}{2} |\nabla h|^2 dx + V(h). \quad (13)$$

with degenerate mobility  $m(h)$ . The thin-film framework is powerful, since it can describe many wetting and dewetting flows quantitatively, e.g., [29] and [P9] and [P4], while maintaining the mathematical complexity of the a free boundary problem [30]. Considerable work was devoted to the study of global solutions, where  $h$  is nonnegative and defined on the entire domain and where algorithms ensure these properties [31, 32]. However, as also suggested by analytical results in [30] and introduced as a numerical algorithm in [P8], the problem should be interpreted as a free boundary problem, where the support set  $\omega(t) = \{x \in \mathbb{R}^{d-1} : h(t, x) > 0\}$  depends on time and evolves due to a kinematic condition. We call corresponding solutions  $(h, \omega)$  of the thin-film equation also **supported solutions**. Alternative approaches regularize the energy by replacing  $V$  by a *precursor potential*  $V_\delta(h) = \int (-S) W(h/\delta) dx$  where  $W(h) = 1 + (m-n)^{-1}(mh^{-n} - nh^{-m})$  and thereby remove the nonsmoothness of  $V(h) = (-S)|\omega|$ . While the degeneracy of  $m(h) \sim h^\sigma$  ( $0 < \sigma < 3$ ) in (13) is sufficient to ensure nonnegativity of  $h$  [33], these intermolecular potentials  $V(h)$  are often also used to enforce positivity of solutions [34]. Numerical solutions of the regularized problem require local spatial adaptivity as shown in Fig. 6. However, it appears that only supported solutions allow the systematic inclusion of contact line physics and in particular of dynamic contact angles into a long-wave framework [P3].

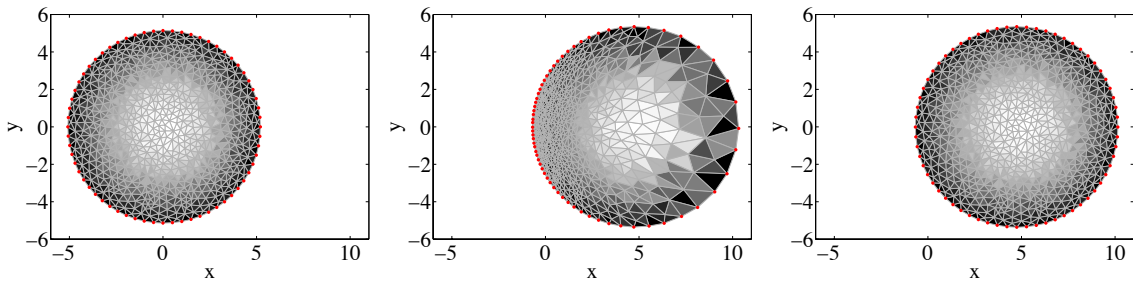


**Figure 5:** Harmonic ALE mesh motion (**left**) starting point at  $t = 0$  and (**middle**) at final position  $t = 14$  transport purely in normal direction deteriorates the mesh but (**right**) with artificial tangential velocity mesh is preserved.

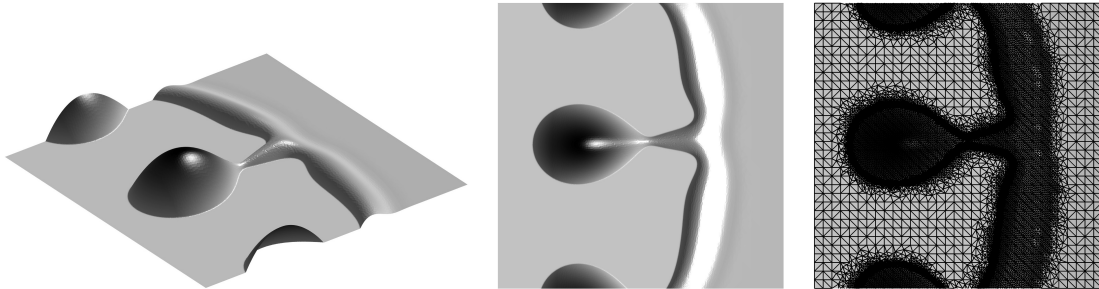


**Figure 6:** Dewetting thin film with regularized energy  $\mathcal{E}_\delta$  (**left**) 3D view of the function  $h(t, x)$  (**middle**) top view and (**right**) top view with locally refined mesh.

**Summary:** Variational methods based on dissipative processes have become an important tool for modeling of complex fluids. But also for simple fluids with complex coupling to substrate dynamics variational methods are essential for coupling of PDEs across interfaces in a consistent manner and to derive advanced models for dynamic contact lines. The author of this proposal has developed several novel theoretical frameworks to model, analyse, and simulate *nonlinearly coupled PDEs* and *free boundary problems*, in particular in the context of thin films.

## 1.1 Project-related publications

### 1.1.1 Articles published by outlets with scientific quality assurance, book publications, and works accepted for publication but not yet published.

- [P1] S. Jachalski, D. Peschka, A. Münch, and B. Wagner, “Impact of interfacial slip on the stability of liquid two-layer polymer films,” *J. Eng. Math.*, vol. 86, 2014.
- [P2] A. Mielke, D. Peschka, N. Rotundo, and M. Thomas, “On some extension of energy-drift-diffusion models: Gradient structure for optoelectronic models of semiconductors,” *Prog. Ind. Math. at ECMI 2016*, vol. 26, 2017.
- [P3] D. Peschka, “Variational approach to contact line dynamics for thin films,” *Phys. Fluids*, vol. 30, 2018.
- [P4] D. Peschka, S. Bommer, S. Jachalski, R. Seemann, and B. Wagner, “Impact of energy dissipation on interface shapes and on rates for dewetting from liquid substrates,” *Sci. Reports*, vol. 8, 2018.
- [P5] R. Huth, S. Jachalski, G. Kitavtsev, and D. Peschka, “Gradient flow perspective on thin-film bilayer flows,” *J. Eng. Math.*, vol. 94, 2015.
- [P6] S. Jachalski, R. Huth, G. Kitavtsev, D. Peschka, and B. Wagner, “Stationary solutions of liquid two-layer thin-film models,” *SIAM J. on Appl. Math.*, vol. 73, 2013.
- [P7] S. Jachalski, D. Peschka, S. Bommer, R. Seemann, and B. Wagner, “Structure formation in thin liquid-liquid films,” in *Transport Processes at Fluidic Interfaces*, Springer, 2017.

- [P8] D. Peschka, "Thin-film free boundary problems for partial wetting," *J. Comput. Phys.*, vol. 295, 2015.
- [P9] S. Bommer, F. Cartellier, S. Jachalski, D. Peschka, R. Seemann, and B. Wagner, "Droplets on liquids and their journey into equilibrium," *The Eur. Phys. J. E*, vol. 36, Aug 2013.

### 1.1.2 Other publications

- [O1] D. Peschka, S. Haefner, K. Jacobs, A. Münch, and B. Wagner, "Signatures of slip in dewetting polymer films," *WIAS preprint No. 2538*, 2018.

## 2 Objectives and work programme

### 2.1 Anticipated total duration of the project

The work programme is composed for a duration of three years starting October 1st, 2019.

### 2.2 Objectives

In this work the proposer's existing results for modeling and simulation using ALE formulations for flows on substrates with dynamic contact angles will be extended to hysteretic motion. The main approach that will be employed is the modeling of dissipative effects in the substrate, on interfaces, and at contact lines. In the long-wave approximation, a framework for the strongly coupled evolution of substrate/interface species and Newtonian bulk flow will be developed. In particular, existing state-of-art results will be extended to include dynamic contact lines using the concept of *supported solutions*. This framework will then be transferred to applications in other projects of the Priority Programme: Pattern formation in dewetting flows, flows over porous substrates, surfactant transport, and the modeling of soft substrates. The common main focus will be the extension to variational formulations with strong coupling of flow and substrate physics.

### 2.3 Work programme incl. proposed research methods

**WP1:** Development of advanced theoretical and numerical methods for long-wave modelling with moving contact lines as the basis for multiphysics models to be used within the SPP.

**Planned Cooperation:** Prof. Axel Voigt (internal, Dresden), Prof. Arnold Reusken (internal, Aachen) Prof. Holger Stark (internal, Berlin), Prof. Uwe Thiele (internal, Münster), Prof. Luca Heltai (external, SISSA, Trieste, Italy).

**Task WP1-1:** *Develop macroscopic long-wave theory and models with moving contact lines to 2D/3D flows with contact angle dynamics with smooth and hysteretic behaviour. (3 months)*

**Description WP1-1:** While the modeling basis for the long-wave theory with contact lines has been described in [P3], the extension to a variational framework including hysteretic contact line motion remains open, even for Stokes flows. Therefore, we will devise different dissipation mechanisms at contact lines, which create physically realistic models for dynamic contact angles, e.g., see [35, 9]. To achieve this task, the strategy of this proposal within the SPP will be two-fold: Firstly, as a proof-of-principle a 2D Stokes flow/thin-film flow solver, which implements contact line dynamics with hysteresis based on generalized gradient flows, will be developed. This will require to solve the nonsmooth convex minimization problem

$$\min_{\mathbf{v} \in V} \left( \frac{1}{2} \mathcal{D}(\mathbf{v}) + \mathcal{J}(\mathbf{v}) + \langle D\mathcal{E}, \mathbf{v} \rangle \right), \quad (14)$$

which transforms the original PDE formulation into a subdifferential inclusion for the nonsmooth contribution to the dissipation  $\mathcal{J}$  and can be solved by relaxation, augmented Lagrangian techniques, or dualization. Similar methods are popular for flows of Bingham fluids, e.g. cf. [36],

and should be adaptable to this situation. In this task, different methods to solve the nonsmooth problem will be investigated. Furthermore, the formal thin-film reduction will be performed and the corresponding variational structure will be investigated. It will be examined if the resulting problem also has a generalized gradient flow structure, *i.e.*, it can also be written as a nonsmooth (convex) minimization problem. The identification of such a structure will later be useful for the development of advanced numerical methods. Methods for the convex nonsmooth optimization (the generalized gradient flow (14)) will be discussed with M. Hintermüller and T. Surowiec.

**Task WP1-2:** *Develop finite-element based tools to solve these problems using higher-order methods in space and time with sharp-interface ALE methods. (6 months)*

**Description WP1-2:** The first goal of the task WP1-2 is to develop the numerical tools for WP1-1, which then serve as the basis for the remaining tasks, where the dissipative substrate-flow coupling will be implemented. In two spatial dimensions, this amounts to generalizing the numerical code published alongside [P3] to deal with hysteresis in the sense of (14). As the corresponding numerical algorithm is devised to be versatile and simple, it is intended to provide it to a software pool within the SPP, which can be used to advance and discuss numerical methods for contact line motion (and to teach to PhD students). This is also relevant, since nonsmooth PDE settings are not commonly used in the physics community. This implies, in particular, that several strategies for solving the nonsmooth (convex) minimization problem will be also presented and compared numerically. The second goal is to extend these methods to higher dimensions, similar to the methods presented in [P8]. Therefore, the plan of WP1-2 is to include the corresponding algorithm into the FEM library deal.II (<https://dealii.org>), which is work in progress with Luca Heltai, one of the maintainers of this library. The deal.II library provides various mapped finite elements, which therefore allows to develop higher-order methods for problems with moving domains. Some preliminary work in this direction has already become part of deal.II version 9.0.0. The main ingredients to be developed for this purpose is an efficient ALE mesh motion strategy, where maps and the problem finite-element formulation are adjusted to produce a higher-order (isoparametric) PDE formulation.

**Task WP1-3:** *Develop a benchmark for free boundary problem with dynamic contact angles to numerical predictions of other groups within the SPP. (1 month)*

**Description WP1-3:** Within the SPP, several numerical approaches to solve flow problems with free boundaries and contact lines are envisioned, *e.g.*, Arnold Reusken (level set based unfitted finite-element method), Holger Stark (boundary element method), Axel Voigt (phase field methods), and the ALE approach of this proposal (for Stokes and thin-films). The goal of WP1-3 is to define models and benchmarks suited for model validation for all these approaches and including dynamic contact angles. As the work of this proposal is more focussed on thin-films, the corresponding numerical method will be extended to encode the full surface energy, which will give rise to the full mean-curvature instead of the Laplacian in the thin-film equation. In the energetic-variational approach this directly generalizes the dynamic contact angle to the corresponding full evolution law. With Uwe Thiele we will compare supported thin-film solutions (and Stokes) with solutions from precursor approaches (full curvature). As part of the preliminary work, also a 2D Taylor-Hood based solver for the Stokes free boundary problem was developed and contains a dynamic contact angle implementation. It is envisioned to extend this work to a full 3D Stokes solver with isoparametric P2-FEM using an ALE-based mesh motion algorithm.

**WP2:** Extension of the long-wave toolbox to a unified theoretical framework of coupled multiphase reactive transport with moving contact lines, where constituents are defined separately in the fluid, in the substrate, on interfaces, or at contact lines.

**Planned Cooperation:** Prof. Uwe Thiele (internal, Münster), Dr. Georgy Kitavtsev (external, Oxford)

**Task WP2-1:** Extension of the existing framework for mass exchange of bulk and interface to mass exchange across (and affecting) contact lines. (4 months)

**Description WP2-1:** The goal of this work package is to develop a general framework for multiphase transport with moving contact lines, where different means of substrate coupling will be investigated, e.g. cf. [37, 38, 39]. In order to be able to highlight the subtleties of the intended approach, in the following a more detailed account of the modeling approach for this task will be given. A long-wave binary mixtures flow with bulk-concentration  $0 \leq \theta \leq 1$  and film height  $h \geq 0$  involves the vector of transported quantities<sup>3</sup>  $\mathbf{c} = (h, w)$  such that

$$\partial_t \mathbf{c} - \nabla \cdot \left( \mathbb{M}(\mathbf{c}) \nabla \frac{\delta \tilde{E}}{\delta \mathbf{c}} \right) = -\mathbb{G}(\mathbf{c}) \frac{\delta \tilde{E}}{\delta \mathbf{c}}. \quad (15)$$

where  $w = h\theta$  and we have additional boundary conditions. From the modeling point-of-view one can write the energy either  $\tilde{E}(\mathbf{c})$  or  $E(h, \theta)$  and derivatives of  $E$  transform as

$$\pi_h := \frac{\delta}{\delta h} \tilde{E} = \left( \frac{\delta}{\delta h} - \frac{\theta}{h} \frac{\delta}{\delta \theta} \right) E, \quad \pi_w := \frac{\delta}{\delta w} \tilde{E} = \frac{1}{h} \frac{\delta}{\delta \theta} E.$$

A large class of energies, which are important for this type of problem, are of the form

$$E(h, \theta) = \int_a^b \frac{1}{2} |\nabla h|^2 + s(\theta) + h f(h, \theta; x) + \frac{1}{2} \gamma h |\nabla \theta|^2 dx,$$

and  $\mathbb{G}, \mathbb{M} \in \mathbb{R}^{2 \times 2}$  above in (15) are symmetric positive semidefinite. A detailed account of the interpretation of the different *bulk contributions* can be found in [40, 41]. If one considers reaction of the constituents  $\theta$  and  $1 - \theta$  with total volume being conserved and a decomposition into convective and diffusional transport, the following choice is found often

$$\mathbb{G}(\mathbf{c}) = \begin{pmatrix} 0 & 0 \\ 0 & g(h, \theta) \end{pmatrix}, \quad \mathbb{M}(\mathbf{c}) = m(h, \theta) \begin{pmatrix} 1 & \theta \\ \theta & \theta^2 \end{pmatrix} + \begin{pmatrix} 0 & 0 \\ 0 & d(h, \theta) \end{pmatrix}.$$

so that the only unknown material laws are the scalar functions  $s, f$  and  $g, m, d \geq 0$ . This bulk Onsager structure is well-known [42]. In the SPP, I will consider general classes of mobility matrices  $\mathbb{M}$ , e.g., to facilitate surfactant transport or transport into porous substrates [43]. Also, we will consider *supported solutions*, i.e., we seek the contact line positions  $a(t) < b(t)$  such that  $h(t, \cdot) > 0$  on  $(a(t), b(t))$  and  $h(t, a(t)) = h(t, b(t)) = 0$ . Additionally, for the SPP the inclusion of (sharp) contact line dynamics is important and not considered in the literature. Therefore, in addition to the statement of (15) (with boundary conditions) it is postulated that energy is dissipated according to the balance

$$\frac{d}{dt} \tilde{E}(\mathbf{c}(t)) = -D(\dot{\mathbf{c}}) := - \sum_{i,j=1}^2 \left[ \int_a^b \mathbb{M}_{ij} \nabla \pi_i \nabla \pi_j + \mathbb{G}_{ij} \pi_i \pi_j dx + \int_{\partial[a,b]} \mathbb{R}_{ij} \pi_i \pi_j \right] \leq 0.$$

<sup>3</sup>**Note:** Conventionally one would use transport equations for  $c_1 = \theta$  and  $c_2 = 1 - \theta$ . However, instead we write transport equation for  $\theta$  (total amount of  $c_1$ ) and  $h$  (total volume  $c_1 + c_2$ ).

with a new contribution  $\mathbb{R}(\mathbf{c})$  at the contact line. In order for the total volume to be conserved, we define this contact line reaction term by

$$\mathbb{R}(\mathbf{c}) = \begin{pmatrix} 0 & 0 \\ 0 & r(\mathbf{c}) \end{pmatrix},$$

which is constructed using  $r(\mathbf{c}) \geq 0$  and more general choices of  $\mathbb{R}(\mathbf{c})$  are possible (symmetric, positive semidefinite). In addition to (15), this creates another boundary reaction-term in the  $\theta$ -transport equation. The kinematic condition corresponding to  $h(t, a) = h(t, b) = 0$  is

$$\dot{h} + \dot{a} \cdot \nabla h = 0 \quad \text{and} \quad \dot{h} + \dot{b} \cdot \nabla h = 0, \quad (16)$$

at  $x = a$  and  $x = b$ , respectively. Evaluating (15) and the energy-dissipation balance above produces the multiphase flow equations with mass transport at the contact line. While many works consider Onsager structures for bulk processes, the proposed work will extend this approach and consider dissipation on interfaces and at contact lines, so that flow-substrate coupling can be introduced in a systematic manner. For the application within the SPP, this approach will be further extended in several aspects: the solution vector  $\mathbf{c}$  will include quantities (densities, energies, etc.) defined outside the fluid support  $(a, b)$  and defined in the substrate; further state-dependent dissipation terms at the contact line will be added to include contact angle dynamics. The gradient flow approach constructed here is somewhat similar to the approach used for liquid substrates [P5] but extended due to the concept of reactive flow presented above.

The goal of the task WP2-1 is to extend the variational framework to reactive mass transport starting with the binary case, where the particular novelty will be the coupling of mass transport to sharp contact lines and including nontrivial contact line dynamics. Formal asymptotics similar to [44] will show if the mathematical model, *i.e.*, in particular the contact line dynamics, is admissible. Since also similar Stokes models for binary mixtures exist, *e.g.*, [45], we will also perform the long-wave approximation in order to find regimes with possibly novel transport laws  $\mathbb{M}(\mathbf{c})$  in the strongly coupled cases where  $\theta \rightarrow \theta_{\text{crit}} \leq 1$ . In particular for multiphase flows of (non-colloidal) suspensions there is active research in the direction of understanding jamming transitions, normal pressures, and shear induced migration [46, 47, 48], which is also an interesting application of the strong-coupling, *e.g.*, influence of suspension density on dewetting in Fig. 9. Similar models also play a role in cell-motility problems [44]. In order to couple the fluid flow to an elastic deformable substrate, we will consider the inclusion of algebraic equation into the gradient flow. This is similar to the role of the electrostatic potential in the gradient flow construction for the van Roosbroeck system for charge transport in semiconductors, which is presented in [P2].

The discussion of the bulk-thermodynamics for the reactive transport framework with contact lines is planned to be in cooperation with Uwe Thiele, with a particular focus also on mixtures and surfactant flows. The related application to cell-motility problems will be investigated with Georgy Kitavtsev.

**Task WP2-2:** Develop a general numerical finite-element based framework for fluid-substrate coupling with moving contact lines. (4 months)

**Description WP2-2:** The bulk part of the degenerate parabolic equation is rather standard to implement [34, 49] or [O1]. While the mathematical long-wave theory for the corresponding problem with moving contact lines has been developed in the last years [30, 50], the construction of corresponding versatile numerical algorithms was done in [P8, P3] and [51]. For the topic of surfactant transport and substrate interaction the work by Karapetsas et al. [52] is a notable mention for coupled systems. However, in the proposer's understanding the numerical approach in

that paper lacks the necessary versatility, which the gradient flow approach based on functionals supplied in [P5] delivers.

Therefore, the goal of WP2-2 is to develop a toolbox of FE methods needed to solve problems similar to [P5], where different types of substrate dissipation mechanisms are coupled to contact line dynamics. Possible routes for implementation of the coupling are:

- (mapped) finite-elements for multiphysics problems: degrees of freedom on subdomains; jumps across interfaces; PDEs on interfaces; Lagrange multipliers,
- (classical) numerical strategies for coupling in multiphysics problems: Mortar elements; Lagrange multipliers; domain decomposition; time-splitting,
- time-discretization schemes: explicit/implicit; higher-order; stabilization,
- advance ALE methods from WP1 to flow-substrate coupling (rigid vs elastic substrates).

This toolbox development is also explorative, since the choice of method will certainly depend on the type of considered coupling. While for liquid substrates as considered in [P5] the strong coupling required to solve the fully coupled system in a monolithic way, for fluid-structure interaction problems also splitting or iterative methods can be feasible, e.g., see for Stokes flow [53, 54].

### WP3: Transfer of the developed methodologies within the SPP and externally.

**Planned Cooperation:** Prof. B. Rapp/Dr. D. Helmer (internal, Karlsruhe Institute of Technology), Prof. U. Thiele (internal, Münster), Dr. M. Brinkmann (internal, Saarbrücken), Prof. R. Seemann/Prof. B. Wagner (internal, Saarbrücken & Berlin), Prof. Karin Jacobs (external, Saarbrücken), Prof. Alexander Mielke (external, Berlin)

#### Task WP3-1: Control and pattern formation of fluid flow by effective, heterogeneous, and switchable substrates. (6 months)

**Description WP3-1:** The goal of the task to apply the previously developed simulation tools to the experimental situations considered in the SPP. Therefore, the algorithms developed in WP1 and the model framework considered in WP2 will be extended to account for heterogeneous (in space) and switchable (in time) substrate properties. In general, wetting and dewetting of (chemically) heterogeneous substrates with precursor approaches is well studied [55, 56, 57] and is also confirmed experimentally, e.g. [58]. An example for dewetting from a heterogeneous substrate with supported solutions is shown in Fig. 7, where the spreading coefficient is inhomogeneous, so that it is energetically favorable to cover the green instead of the red areas. The corresponding surface energy is

$$E_{\text{surf}}(h) = \int_{\omega} \frac{1}{2} |\nabla h|^2 + f(h, x) dx, \quad (17)$$

where  $f(h, x) \geq 0$  encodes space-dependent surface (and bulk) energy. In this example a gravity-type force is additionally used to move the droplet over the energetic texture. The advantage of the proposed approach is that within the energetic gradient formulation such a modification is straight-forward to implement. Other properties which will be changed to control of fluid flow are: *modification of magnitude and mechanism for substrate-flow interface condition, anisotropy of substrate-flow slip, oscillating surface energy (roughness and microstructure) and chemically textured surfaces* as shown above. These interface properties can depend on space (heterogeneous) and time (switchable).

With respect to the experiments provided by the groups within the SPP, this should provide effective and viable routes for free surface flow control and the proposed methods should be able to effectively describe the intended physical behavior of moving contact lines. In cooperation with Bastian Rapp & Dorothea Helmer I plan to perform a joint simulation/experimental description

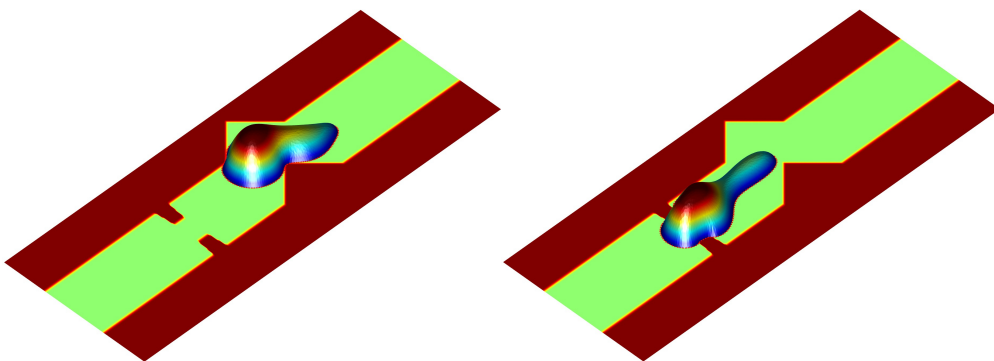


**Figure 7:** Supported droplet (shading=height) driven over a chemically heterogeneous substrate landscape.

of droplets moving over patterned/functionalized surface [59, 60]. The droplet motion (height and contact line) will be monitored using a high-speed camera and compared with the simulation results. The goal of this study is to indirectly identify/verify physical parameters such as interface slip and dynamic contact angle. Even for homogeneous substrates, the magnitude of the dissipation mechanism can drastically influence the observed pattern formation process, e.g. cf. [O1] for a systematic study concerning the magnitude of Navier-slip. With the development of the theoretical and numerical framework for dynamic contact angles in WP1, a similar study for dewetting films and the created patterns will be performed in this proposal and compared with experimental results from the group of Karin Jacobs, e.g. cf. [61] & [O1]. For preliminary result of such a simulation with sharp contact lines but with equilibrium contact angles is shown in Fig. 8. Concerning the quasi-static evolution of gravity-driven droplets I will work with Martin Brinkmann to investigate the impact of different (gradient formulations) for dynamic contact angle on observed droplet and join the approaches of [62] and [P3].

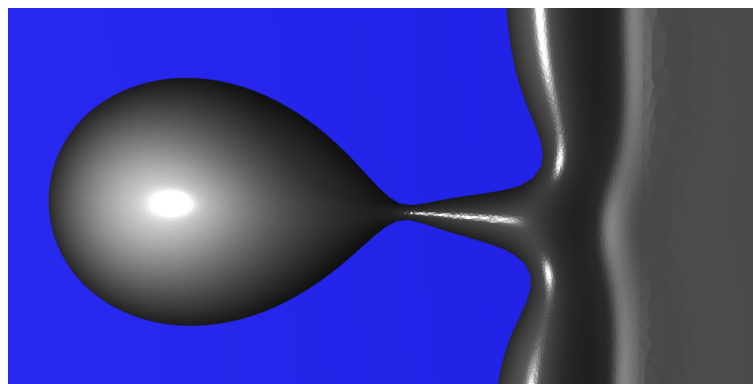


**Figure 8:** Droplet pinch-off from a dewetting liquid computed using supported solutions (blue=outside support).

**Task WP3-2: Models for flows over and into porous substrates (4 months).**

**Description WP3-2:** On the full hydrodynamic level, the substrate-flow interaction with a porous substrate is well-known and described by the Stokes-Darcy equation [37]. The numerical strategy to couple these equations, for example, was investigated in [63] and its impact on the spreading dynamics has been studied in [38]. In particular in relation with the previous task WP3-1, we will study how transport of fluid into the porous substrate impacts the interface properties (interface energies, Navier-slip, hysteresis) and how this can be observed in the corresponding dynamic behavior of the spreading/dewetting process. Additionally, valuable information about the coupled flow will be extracted, if the flow in the porous substrate can be at least partially observed experimentally, e.g., velocity of internal liquid front. In cooperation with Bastian Rapp & Dorothea

Helmer we also plan to investigate the transport of fluid into a porous substrate, e.g. produced as in [64]. In the experiment, fluorescently marked water will be introduced into a porous polymer and the spreading of the water on the substrate and into the substrate will be tracked by fluorescence microscopy in 2D and by confocal microscopy in 3D to provide experimental insight on spreading dynamics. We will compare with models and simulations developed within this proposal to study if such models are useful for predicting substrate properties such as pore sizes from spreading data by applying a fitting theoretical model. With Martin Brinkmann I will investigate the dynamics and wetting of flows on elastic posts and the flow into these porous structures. Depending their characteristic length scale and wetting properties, we claim that dynamical transitions between Cassie-Baxter-like and Wenzel-like states can be observed, which we will then describe in thermodynamic consistent manner. Following experimental evidence, we will particularly focus on investigating hysteretic behavior in the substrate dynamics.

Assume a porous/heterogeneous substrate gives rise to a microscopically oscillating surface energy where  $f_\varepsilon(h, x) = g(x/\varepsilon)$  with a 1-periodic function  $g : [0, 1]^d \rightarrow \mathbb{R}^+$ . Upon homogenization the energy converges to the mean spreading coefficient  $f_\epsilon(h, x) \rightarrow \int_{[0,1]^d} g(y) dy \in \mathbb{R}$  as  $\varepsilon \rightarrow 0$ , while the limit for the (sharp interface) evolution is still an open problem. While for models with precursor pinning has been observed [56], the behavior of the moving contact line should be investigated in more detail (numerically and mathematically). There are hints how hysteresis can emerge from such a limit mathematically [65], which will be investigated with Alexander Mielke.

#### **Task WP3-3:** *Model surfactant transport (soluble and insoluble) (4 months).*

**Description WP3-3:** A natural physical setting corresponding to WP2 is the study of surfactant dynamics for soluble and insoluble surfactants distributed on surfaces, substrate-liquid interface, and in the liquid bulk. For an overview concerning surfactant assisted spreading we refer to Matar & Craster [66]. Corresponding models have been analysed in [67] and phase-field variants considered in [68]. A 1D thin-film model with moving contact lines and surfactants has been considered in [52]. However, the advantage of a gradient flow formulation with moving contact lines, which the current proposal is concerned with, is that all natural boundary conditions are derived from energy or dissipation functionals. Onsager structures for the flow with surfactants have been studied in [40] and their hydrodynamical stability investigated in [69].

In the SPP, the first part of the task WP3-3 I will focus on the theoretical derivation and formalization of a gradient flow structure for a surfactant transport model with moving contact lines and nontrivial contact angle dynamics. This will be studied in a joint effort with Uwe Thiele, who will investigate similar models from the perspective of bulk/interface substrate-flow coupling with adaptive brushes. The theoretical contributions are complementary with my focus on generalized gradient flows with moving contact lines (supported solutions with hysteresis), where Uwe Thiele's focus is on Onsager-structures with adaptive brushes. The development of corresponding advanced numerical algorithms should allow a rich discussion and creation of benchmark studies within the SPP. Jointly, Georgy Kitavtsev (Univ. Oxford), I will also work on extension of this framework to cell-motility, e.g. cf. [44]. This task is the practical application of WP2-1, so that there is the possibility to interchange the (timely) order of tasks in WP2 and WP3.

#### **Task WP3-4:** *Modeling of elastic/deformable substrates with moving contact lines (4 months).*

**Description WP3-4:** Based on the theoretical work on the dissipation modeling for suspension two-phase flows [23], this workpackage uses a similar flow-map based approach for a dissipative fluid-solid coupling. We will model the quasi-static evolution with a dissipation in the fluid  $\Omega$  and

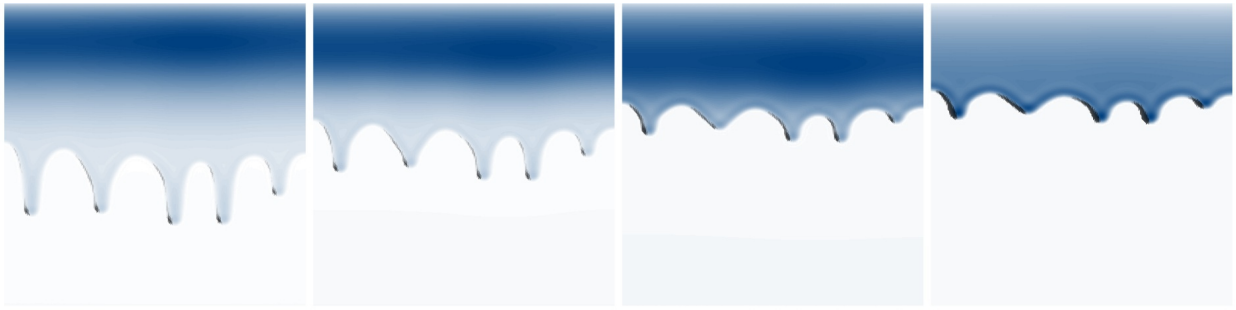


**Figure 9:** Simulation of gravitational fingering instability of a suspension flow as in Eq. (15) on inclines with angles increasing from left to right and density indicated by the shading. Numerical method is based on gradient flow.

the solid  $\bar{\Omega}$

$$\mathcal{D}(\mathbf{u}_\ell, \dot{\mathbf{u}}_s) = \int_{\bar{\Omega}} R_{\text{visc}}(\mathbb{D}\dot{\mathbf{u}}_s) \, dx + \int_{\Gamma} R_\Gamma(\dot{\mathbf{u}}_s - \mathbf{u}_\ell) \, ds + \int_{\Omega} \boldsymbol{\tau}(\mathbf{u}) : \nabla \mathbf{u} \, dx,$$

where  $\mathbf{u}$  is the fluid velocity and  $\mathbf{u}_s$  is the solid deformation velocity. The most natural interface condition would emerge from  $R_\Gamma(w) = \mu_\Gamma |w|^2$  and gives rise to a Navier-slip condition and  $R_{\text{visc}}$  gives rise to viscoelastic material behavior. In the presence of a moving contact line the dissipation  $R_{\text{visc}}$  leads to a localization of the dissipation at the contact line [70] and thereby should create an effective law for a dynamic contact line. The elastic energy will, as usual, be given in Lagrangian coordinates as  $\mathcal{E}_{\text{elast}}(\mathbf{u}_s) = \int_{\bar{\Omega}_{\text{ref}}} W_{\text{elast}}(F) \, dx_{\text{ref}}$  with the deformation gradient  $F = \nabla_{\text{ref}} \mathbf{u}_s$ . This modeling approach will be used to work with Barbara Wagner and Ralf Seemann on dissipative effects in coupling flow with soft elastic substrates. This will allow us to systematically study the effect of viscoelastic dissipation, e.g., cf. [71], in particular studying its impact on the effective contact line dynamics and thereby its impact on the overall dewetting process. Martin Brinkmann studies the effective dynamics and pattern formation of droplet arrays between arrays of elastic lammelas. We will cooperate on aspects of the consistent coupling and on the emergence of hysteretic behavior by dissipation modeling due to contact line dynamics.

## 2.4 Data handling

Research data at WIAS is subject to frequent backups and kept for at least 10 years. Software developed in all work packages will be documented and published, e.g., as in the repository <https://github.com/dpeschka/thinfilm-freeboundary> from [P8]. Publishing data is supported by WIAS by providing DOIs and storage capacity, e.g., see the work [21] featuring research data published at [www.wias-berlin.de/resdata/3/](http://www.wias-berlin.de/resdata/3/).

## 2.5 Other information

none.

## 2.6 Descriptions of proposed investigations involving experiments on humans, human materials or animals as well as dual use research of concern

none.

## 2.7 Information on scientific & financial involvement of international cooperation partners

none.

## 2.8 Information on scientific cooperation within Priority Programme

To foster the exchange between theoretical groups working with continuum-theoretical approaches within the SPP, we have initiated an informal network, which at the moment includes **M. Brinkmann**, **S. Gurevich**, **D. Peschka**, **J. Snoeijer**, **H. Stark**, **U. Thiele**, **A. Voigt** and **B. Wagner** and which is open to others. There, we will coordinate aspects of the training of the involved young researchers within the SPP, and meet sporadically to discuss details of our approaches and ongoing work. Several groups in the SPP are working on numerical algorithms for flows on rigid (**A. Voigt**, **A. Reusken**, **S. Aland**, **H. Stark**) and agreed to define numerical benchmark problems, where also dynamic contact angles will be considered. With **B. Rapp & D. Helmer** we plan to compare experiments and simulations for chemically structured substrates. With **U. Thiele** I will investigate the coupling of long-wave multiphase transport and nontrivial contact angle dynamics. With **B. Wagner** and **R. Seemann** we will discuss dissipative substrate-flow coupling for soft substrates. With **M. Brinkmann** I will work on hysteresis for soft and porous substrates.

## 3 Bibliography

- [1] L. Onsager, “Reciprocal relations in irreversible processes. i.”, *Phys. Rev.*, 37, 1931.
- [2] S. R. De Groot and P. Mazur, *Non-equilibrium thermodynamics*. Courier Corporation, 2013.
- [3] M. A. Peletier, “Variational modelling: Energies, gradient flows, and large deviations”, *arXiv preprint arXiv:1402.1990*, 2014.
- [4] C. Huh and L. Scriven, “Hydrodynamic model of steady movement of a solid/liquid/fluid contact line”, *J. Colloid Interface Sci.*, 35, 1971.
- [5] E. Lauga, M. Brenner, and H. Stone, “Microfluidics: The no-slip boundary condition”, in *Springer Handbook of Experimental Fluid Mechanics*, Springer, 2007.
- [6] A. Münch, B. Wagner, and T. P. Witelski, “Lubrication models with small to large slip lengths”, *J. Eng. Math.*, 53, 2005.
- [7] Y. D. Shikhmurzaev, “Moving contact lines in liquid/liquid/solid systems”, *J. Fluid Mech.*, 334, 1997.
- [8] D. Bedeaux, “Nonequilibrium thermodynamic description of the three-phase contact line”, *The J. Chem. Phys.*, 120, 2004.
- [9] J. H. Snoeijer and B. Andreotti, “Moving contact lines: Scales, regimes, and dynamical transitions”, *Annu. Rev. Fluid Mech.*, 45, 2013.
- [10] D. Bonn, J. Eggers, J. Indekeu, J. Meunier, and E. Rolley, “Wetting and spreading”, *Rev. Mod. Phys.*, 81, 2009.
- [11] A. Cassie and S. Baxter, “Wettability of porous surfaces”, *Transactions Faraday society*, 40, 1944.
- [12] R. Cox, “The dynamics of the spreading of liquids on a solid surface. Part 1. Viscous flow”, *J. Fluid Mech.*, 168, 1986.
- [13] T. Blake and J. Haynes, “Contact-angle hysteresis”, *Prog. Surf. Membr. Sci.*, 6, 1973.
- [14] W. Ren and W. E, “Boundary conditions for the moving contact line problem”, *Phys. Fluids*, 19, 2007.
- [15] F. Otto, “The geometry of dissipative evolution equations: The porous medium equation”, *Commun. Partial. Differ. Equations*, 26, 2001.
- [16] A. N. Beris and B. J. Edwards, *Thermodynamics of flowing systems: with internal microstructure*. 36, Oxford University Press on Demand, 1994.
- [17] M. Grmela and H. C. Öttinger, “Dynamics and thermodynamics of complex fluids. I. Development of a general formalism”, *Phys. Rev. E*, 56, 1997.
- [18] M.-H. Giga, A. Kirshtein, and C. Liu, “Variational modeling and complex fluids”, *Handb. Math. Analysis Mech. Viscous Fluids*, 2018.

- [19] P.-G. De Gennes, "Wetting: Statics and dynamics", *Rev. Mod. Phys.*, 57, 1985.
- [20] A. Mielke, "Formulation of thermoelastic dissipative material behavior using GENERIC", *Continuum Mech. Thermodyn.*, 23, 2011.
- [21] P. Farrell and D. Peschka, "Challenges for drift-diffusion simulations of semiconductors: A comparative study of different discretization philosophies", *WIAS preprint 2486*, 2018.
- [22] K. Kostourou, D. Peschka, A. Münch, B. Wagner, S. Herminghaus, and R. Seemann, "Interface morphologies in liquid/liquid dewetting", *Chem. Eng. Process. Process. Intensif.*, 50, no. 5-6, pp. 531–536, 2011.
- [23] D. Peschka, M. Thomas, T. Ahnert, A. Münch, and B. Wagner, "Gradient structures for flows of concentrated suspensions", *WIAS preprint No. 2543*, 2018.
- [24] J. Lowengrub and L. Truskinovsky, "Quasi-incompressible Cahn-Hilliard fluids and topological transitions", *Proceedings: Math. Phys. Eng. Sci.*, 454, 1998.
- [25] F. Montefuscolo, F. S. Sousa, and G. C. Buscaglia, "High-order ALE schemes for incompressible capillary flows", *J. Comput. Phys.*, 278, 2014.
- [26] E. Bänsch, "Finite element discretization of the Navier–Stokes equations with a free capillary surface", *Numer. Math.*, 88, 2001.
- [27] T. Wick, "Fluid-structure interactions using different mesh motion techniques", *Comput. & Struct.*, 89, 2011.
- [28] L. Giacomelli and F. Otto, "Rigorous lubrication approximation", *Interface. Free. Bound.*, 5, 2003.
- [29] A. Oron, S. H. Davis, and S. G. Bankoff, "Long-scale evolution of thin liquid films", *Rev. Mod. Phys.*, 69, 1997.
- [30] H. Knüpfer, "Well-posedness for a class of thin-film equations with general mobility in the regime of partial wetting", *Arch. for Ration. Mech. Analysis*, 218, 2015.
- [31] G. Grün and M. Rumpf, "Nonnegativity preserving convergent schemes for the thin film equation", *Numer. Math.*, 87, 2000.
- [32] J. A. Diez, L. Kondic, and A. Bertozzi, "Global models for moving contact lines", *Phys. Rev. E*, 63, 2000.
- [33] F. Bernis and A. Friedman, "Higher order nonlinear degenerate parabolic equations", *J. Differ. Equations*, 83, 1990.
- [34] M. Eres, L. Schwartz, and R. Roy, "Fingering phenomena for driven coating films", *Phys. Fluids*, 12, 2000.
- [35] P.-G. de Gennes, "Wetting: Statics and dynamics", *Rev. Mod. Phys.*, 57, 1985.
- [36] E. J. Dean, R. Glowinski, and G. Guidoboni, "On the numerical simulation of Bingham visco-plastic flow: Old and new results", *J. Non-Newtonian Fluid Mech.*, 142, 2007.
- [37] W. J. Layton, F. Schieweck, and I. Yotov, "Coupling fluid flow with porous media flow", *SIAM J. on Numer. Analysis*, 40, 2002.
- [38] V. Starov, S. Zhdanov, S. Kosvintsev, V. Sobolev, and M. Velarde, "Spreading of liquid drops over porous substrates", *Adv. Colloid Interface Sci.*, 104, 2003.
- [39] G. Kumar and K. N. Prabhu, "Review of non-reactive and reactive wetting of liquids on surfaces", *Adv. colloid interface science*, 133, 2007.
- [40] U. Thiele, A. J. Archer, and M. Plapp, "Thermodynamically consistent description of the hydrodynamics of free surfaces covered by insoluble surfactants of high concentration", *Phys. Fluids*, 24, 2012.
- [41] U. Thiele, D. V. Todorova, and H. Lopez, "Gradient dynamics description for films of mixtures and suspensions: Dewetting triggered by coupled film height and concentration fluctuations", *Phys. Rev. Lett.*, 111, 2013.
- [42] X. Xu, U. Thiele, and T. Qian, "A variational approach to thin film hydrodynamics of binary mixtures", *J. Physics: Condens. Matter*, 27, 2015.
- [43] U. Thiele, A. J. Archer, and L. M. Pismen, "Gradient dynamics models for liquid films with soluble surfactant", *Phys. Rev. Fluids*, 1, 2016.
- [44] J. Oliver, J. King, K. McKinlay, P. Brown, D. Grant, C. Scotchford, and J. Wood, "Thin-film theories for two-phase reactive flow models of active cell motion", *Math. Medicine Biol.*, 22, 2005.
- [45] W. Alt and M. Dembo, "Cytoplasm dynamics and cell motion: two-phase flow models", *Math. biosciences*, 156, 1999.

- [46] C. Cassar, M. Nicolas, and O. Pouliquen, "Submarine granular flows down inclined planes", *Phys. fluids*, 17, 2005.
- [47] F. Boyer, É. Guazzelli, and O. Pouliquen, "Unifying suspension and granular rheology", *Phys. Rev. Lett.*, 107, 2011.
- [48] N. Murisic, B. Pausader, D. Peschka, and A. L. Bertozzi, "Dynamics of particle settling and resuspension in viscous liquid films", *J. Fluid Mech.*, 717, 2013.
- [49] L. Kondic and J. Diez, "Pattern formation in the flow of thin films down an incline: Constant flux configuration", *Phys. Fluids*, 13, 2001.
- [50] F. B. Belgacem, M. V. Gnann, and C. Kuehn, "A dynamical systems approach for the contact-line singularity in thin-film flows", *Nonlinear Analysis*, 144, 2016.
- [51] D. Peschka, "Numerics of contact line motion for thin films", *IFAC-PapersOnLine*, 48, 2015.
- [52] G. Karapetsas, R. V. Craster, and O. K. Matar, "On surfactant-enhanced spreading and superspreading of liquid drops on solid surfaces", *J. Fluid Mech.*, 670, 2011.
- [53] S. Badia, A. Quaini, and A. Quarteroni, "Splitting methods based on algebraic factorization for fluid-structure interaction", *SIAM J. on Sci. Comput.*, 30, 2008.
- [54] S. Badia, F. Nobile, and C. Vergara, "Fluid structure partitioned procedures based on robin transmission conditions", *J. Comput. Phys.*, 227, 2008.
- [55] K. Kargupta and A. Sharma, "Templating of thin films induced by dewetting on patterned surfaces", *Phys. Rev. Lett.*, 86, 2001.
- [56] L. Brusch, H. Kühne, U. Thiele, and M. Bär, "Dewetting of thin films on heterogeneous substrates: Pinning versus coarsening", *Phys. Rev. E*, 66, 2002.
- [57] M. Köpf, S. Gurevich, R. Friedrich, and U. Thiele, "Substrate-mediated pattern formation in monolayer transfer: a reduced model", *New J. Phys.*, 14, 2012.
- [58] A. Sehgal, V. Ferreiro, J. F. Douglas, E. J. Amis, and A. Karim, "Pattern-directed dewetting of ultrathin polymer films", *Langmuir*, 18, 2002.
- [59] A. Waldbaur, B. Waterkotte, K. Schmitz, and B. E. Rapp, "Maskless projection lithography for the fast and flexible generation of grayscale protein patterns", *Small*, 8, 2012.
- [60] T. M. Nargang, M. Runck, D. Helmer, and B. E. Rapp, "Functionalization of paper using photobleaching: A fast and convenient method for creating paper-based assays with colorimetric and fluorescent readout", *Eng. Life Sci.*, 16, 2016.
- [61] R. Seemann, S. Herminghaus, and K. Jacobs, "Gaining control of pattern formation of dewetting liquid films", *J. Physics: Condens. Matter*, 13, 2001.
- [62] C. Semprebon and M. Brinkmann, "On the onset of motion of sliding drops", *Soft Matter*, 10, 2014.
- [63] M. Discacciati, A. Quarteroni, and A. Valli, "Robin–robin domain decomposition methods for the stokes–darcy coupling", *SIAM J. on Numer. Analysis*, 45, 2007.
- [64] D. Helmer, N. Keller, F. Kotz, F. Stolz, C. Greiner, T. M. Nargang, K. Sachsenheimer, and B. E. Rapp, "Transparent, abrasion-insensitive superhydrophobic coatings for real-world applications", *Sci. Reports*, 7, 2017.
- [65] A. Mielke, "Emergence of rate-independent dissipation from viscous systems with wiggly energies", *Continuum Mech. Thermodyn.*, 24, 2012.
- [66] O. K. Matar and R. V. Craster, "Dynamics of surfactant-assisted spreading", *Soft Matter*, 5, 2009.
- [67] D. Bothe, J. Prüss, and G. Simonett, "Well-posedness of a two-phase flow with soluble surfactant", in *Nonlinear elliptic and parabolic problems*, Springer, 2005.
- [68] H. Garcke, K. F. Lam, and B. Stinner, "Diffuse interface modelling of soluble surfactants in two-phase flow", *Commun. Math. Sci.*, 12, 2014.
- [69] A. Pereira, P. Trevelyan, U. Thiele, and S. Kalliadasis, "Dynamics of a horizontal thin liquid film in the presence of reactive surfactants", *Phys. fluids*, 19, 2007.
- [70] S. Karpitschka, S. Das, M. van Gorcum, H. Perrin, B. Andreotti, and J. H. Snoeijer, "Droplets move over viscoelastic substrates by surfing a ridge", *Nat. communications*, 6, 2015.
- [71] M. Shanahan and A. Carre, "Viscoelastic dissipation in wetting and adhesion phenomena", *Langmuir*, 11, 1995.

## 4 Requested modules/funds

### 4.1 Basic Module

#### 4.1.1 Funding for Staff

1 full time position E13 TVöD for three years (Eigene Stelle).

#### 4.1.2 Direct Project Costs

5,250 EUR p.a. (see below)

##### 4.1.2.1 Equipment up to €10,000, Software and Consumables

none.

**4.1.2.2 Travel Expenses** Two annual visits of major international conferences (ICIAM, ECMI, APS DFD meeting, Free Boundary Problems Theory and Application) and additional networking activities (see Sec. 2.8) are planned, for which 3,000 EUR p.a. are requested.

**4.1.2.3 Visiting Researchers** External cooperation partners (G. Kitavtsev, L. Heltai) are invited for one week each p.a., for which 1,500 EUR p.a. are requested.

**4.1.2.4 Expenses for Laboratory Animals:** none.

**4.1.2.5 Other Costs:** none.

**4.1.2.6 Project-related publication expenses:** For support of open access publications 750 EUR p.a. are requested.

#### 4.1.3 Instrumentation

**4.1.3.1 Equipment exceeding €10,000:** none.

**4.1.3.2 Major Instrumentation exceeding €50,000:** none.

## 5 Project requirements

### 5.1 Employment status information

Dirk Peschka has a fixed term contract as research assistant until December 31, 2018 funded by Einstein Center for Mathematics Berlin in the MATHEON project *OT8 Modeling, analysis, and optimization of optoelectronic semiconductor devices driven by experimental data*.

### 5.2 First-time proposal data

Does not apply. The applicant was one of the proposers in the DFG SPP 1506 project *Mathematical modeling, analysis, numerical simulation of thin liquid bilayers and validation experiments*.

### 5.3 Composition of the project group

Does not apply.

## 5.4 Cooperation with other researchers

### 5.4.1 Researchers with whom you have agreed to cooperate on this project (external)

**K. Jacobs (Universität des Saarlandes, Saarbrücken)** develops experimental methods for dewetting flows from rigid coated substrates to be probed by AFM. We agreed to compare the developed models with existing experiments for dewetting patterns from coated substrates.

**L. Heltai (SISSA, Trieste)** is an expert in high performance computing with a focus on free boundary and fluid-structure interaction problems. We will jointly develop higher-order ALE methods using mapped finite-elements. We have preliminary results within the deal.ii finite-element library.

**A. Mielke (WIAS, Berlin)** develops analytical methods for evolutionary  $\Gamma$ -convergence based on energetic solution concepts. He showed the emergence of rate-independent dissipation in the homogenization of an evolution problem with microstructure (wiggly energy landscape). We will jointly work on transferring this concept to heterogeneous/rough surfaces.

With **T. Surowiec (Philipps Universität Marburg)** and **M. Hintermüller (WIAS, Berlin)** I will cooperate on nonsmooth variational problems and gradient structures for electrowetting. With **V. John** and **A. Linke (both WIAS, Berlin)** I will discuss the numerical analysis of flow problems. With **M. Thomas (WIAS, Berlin)** I will discuss modeling and analysis of rate-independent systems with elasticity and fracture mechanics and possible applications in geophysics. With **G. Kitavtsev (Univ. of Oxford)** I will work on gradient flow formulations for cell-motility problems.

### 5.4.2 Researchers with whom you collaborated scientifically within the past three years

Ralf Seemann<sup>a</sup>, Karin Jacobs<sup>a</sup> Thomas Surowiec<sup>b</sup>, Patricio Farrell<sup>c</sup> Michael Hintermüller<sup>d</sup>, Barbara Wagner<sup>d</sup>, Marita Thomas<sup>d</sup>, Nella Rotundo<sup>d</sup>, Thomas Koprucki<sup>d</sup>, Alexander Mielke<sup>d</sup>, Ansgret Glitzky<sup>d</sup> Andreas Münch<sup>e</sup>, Georgy Kitavtsev<sup>e</sup>, Andrea Bertozzi<sup>f</sup>, Luca Heltai<sup>g</sup>.

a) Universität des Saarlandes, b) Philipps-Universität Marburg, c) TU Hamburg, d) Weierstrass Institute,

e) University of Oxford, f) University of California Los Angeles, g) SISSA Trieste

## 5.5 Scientific equipment

Infrastructure, office space and all other preconditions for carrying out the proposed work will be granted by WIAS for the whole period of the project. A related declaration is attached to the accompanying letter.

**5.6 Project-relevant cooperation with commercial enterprises:** none.

**5.7 Project-relevant participation in commercial enterprises:** none.

## 6 Additional information

The proposer also submitted a DFG proposal **PE 1782/1-1** entirely devoted to the subject of extending methods known for Bingham flows to study contact line hysteresis, with a more mathematical focus. The goal of this proposal in the Priority Programme is the substrate-flow coupling with energy-dissipation structures, where the influence of hysteresis is also present but not the primary objective.

# CURRICULUM VITAE: DR. DIRK PESCHKA

Dr. rer. nat. Dirk Peschka • Weierstraß-Institut für Angewandte Analysis und Stochastik ([WIAS](#))  
Mohrenstr. 39 • 10117 Berlin • ☎ +49 30 20372 443 • ✉ [peschka@wias-berlin.de](mailto:peschka@wias-berlin.de)  
[www.wias-berlin.de/people/peschka](http://www.wias-berlin.de/people/peschka) • ORCID [0000-0002-3047-1140](#)

## Personal Information

Name	Dirk Peschka
Place & Date of Birth	21.11.1977 in Zossen
Marital status	Married (2 Children)
Citizenship	German
Languages	German (native), English (fluent)



## Current Position

At the moment I am working as a postdoctoral researcher at the Weierstraß-Institut in Berlin, performing project-oriented research in applied mathematics and theoretical physics.

## Research Interests

- Modeling:**
- electronics and optics (e.g. charge transport, semiconductor lasers)
  - soft matter problems (e.g. viscous flows, complex fluids, granular matter)
  - multiphase flows (e.g. reacting mixtures, bilayers)
  - energetic principles and thermodynamics (e.g. multiphysics)
- Simulation:**
- finite element methods (FEM) (e.g. conformal, mixed or higher-order FEM)
  - ALE methods for moving domains (e.g. grids, isoparametric FEM)
  - convection dominated transport (e.g. stable discretization, FV schemes)
  - degenerate problems (e.g. stable higher-order methods)
- Mathematics:**
- nonlinear higher-order partial differential equations (PDEs)
  - variational formulations (e.g. gradient flows and their generalization)
  - free boundary problems and moving contact lines
  - model reduction (e.g. matched asymptotic expansions)

## Education

2008	<b>Ph. D. (Dr. rer. nat.) in Mathematics (magna cum laude)</b> Institut für Mathematik, Humboldt-Universität zu Berlin "Analysis of thin films with slippage"
2005-2008	<b>Scholarship in the DFG Graduate School 1128</b> "Analysis, Numerics, and Optimization of Multiphase Problems"
2004-2005	<b>Scholarship in the DFG Graduate School 271/3-02</b> "Strukturuntersuchungen, Präzisionstests und Erweiterung des Standardmodells der Elementarteilchenphysik"
2004	<b>Diploma (Dipl. Phys.) in Physics (mit Auszeichnung)</b> Institut für Physik, Humboldt-Universität zu Berlin "On the semiclassical structure of QCD—A lattice study at finite temperature"

# CURRICULUM VITAE: DR. DIRK PESCHKA

## — Professional Experience & Research Projects

2014-present	<p><b>Research Associate in the Einstein Center for Mathematics</b></p> <ul style="list-style-type: none"><li>• researcher in MATHEON projects OT1 &amp; OT8 on optical technologies OT8: "Modeling, analysis, and optimization of optoelectronic semiconductor devices driven by experimental data" (June 2017-present, with M. Thomas)</li><li>• OT1: "Mathematical modeling, analysis, and optimization of strained germanium-microbridges" (2014-2017, with M. Thomas, T. Surowiec, A. Mielke, M. Hintermüller)</li><li>• member of MATHEON <a href="#">executive board</a></li><li>• organization WIAS "Halbleiterseminar" &amp; "Materialmodellierungsseminar"</li><li>• co-founded a special interest group on computational electronics within the "European Consortium for Mathematics in Industry" (ECMI)</li><li>• organization minisymposia at applied math conferences (ECM, ECMI, ICIAM)</li><li>• <b>software:</b> semiconductor device simulation and optimization</li></ul>
June-Sept 2014 Sept-Nov 2012 Oct-Nov 2011 July-Oct 2010	<p><b>Invited Visiting Researcher at the University of California Los Angeles</b></p> <ul style="list-style-type: none"><li>• modeling, theory, simulation and experiments of suspension flows (with A. Bertozzi, N. Murisic, B. Pausader, L. Wang)</li><li>• mentor for REU project and lab supervisor for <a href="#">UCLA applied math lab</a></li></ul>
June 2010 - May 2014	<p><b>Research Associate in the DFG Research Center MATHEON</b></p> <ul style="list-style-type: none"><li>• researcher in MATHEON <a href="#">project C10</a> on interface dynamics (with B. Wagner)</li><li>• <b>software:</b> complex fluids and Navier-Stokes flow</li></ul>
June 2010 - May 2016	<p><b>Principal Investigator in Priority Programme 1506</b></p> <ul style="list-style-type: none"><li>• co-PI and project proposer of <a href="#">SPP project</a> (2 funding periods)</li><li>• mentor for Ph. D. thesis of Sebastian Jachalski</li><li>• cooperation with R. Seemann and B. Wagner within tandem project</li><li>• associated to MATHEON as SE-AP15</li><li>• <b>software:</b> thin-film / Stokes flow with free boundaries</li></ul>
April 2008 - June 2010	<p><b>Research Associate in an Industry Project with Océ (a Canon company)</b></p> <ul style="list-style-type: none"><li>• research on flow instabilities in an innovative printing device</li><li>• collaboration with E. Bänsch (Univ. Erlangen) from applied mathematics</li><li>• <b>software:</b> particulate flow in an electrolyte</li></ul>
2005-2008	<p><b>Ph. D. candidate in DFG Research Training Group 1128</b></p> <ul style="list-style-type: none"><li>• advisors Prof. A. Münch (Univ. Oxford) and Prof. B. Niethammer (Univ. Bonn)</li></ul>

# CURRICULUM VITAE: DR. DIRK PESCHKA

---

## — Cooperations

- Prof. Alexander Mielke, Prof. Michael Hintermüller, Dr. Marita Thomas, Dr. Nella Rotundo, Dr. Thomas Koprucki, Dr. Matthias Liero and Dr. Annegret Glitzky (all WIAS)  
Topics: modeling, simulation, optimization, and analysis of semiconductor devices
- Prof. Ralf Seemann and Prof. Karin Jacobs (Univ. d. Saarlandes)  
Topics: modeling, validation, simulation of pattern formation processes in multiphase flows
- Dr. Barbara Wagner (WIAS)  
Topics: modeling, model reduction, formal asymptotics
- Prof. Luca Heltai (SISSA, Trieste)  
Topics: higher-order methods and high-performance computing with the deal.II library
- Dr. Patricio Farrell (Hamburg Univ. of Technology)  
Topics: numerical methods for drift-diffusion semiconductor models
- Prof. Andrea Bertozzi (Univ. of California Los Angeles)  
Topics: simulation, modeling and experiments for suspension flows
- Prof. Andreas Münch and Dr. Georgy Kitavtsev (Univ. Oxford)  
Topics: modeling, asymptotical methods, simulation, applications with fluid flows
- Prof. Thomas Surowiec (Univ. Marburg)  
Topics: topology optimization of optoelectronic devices
- Prof. T. John, Dr. H. Vrijmoed (FU Berlin) and Dr. M. Rosenau (GFZ Potsdam)  
Topics: modeling and simulation of multiscale geophysical systems
- Prof. G. Capellini (IHP Frankfurt Oder), Dr. M. Virgilio (Univ. Pisa), Prof. T. Schröder (IKZ)  
Topics: experiments, modeling, simulation, and optimization of optoelectronic devices

## — Third Party Funding

In cooperation with Dr. Barbara Wagner (WIAS) and Prof. Ralf Seemann (Univ. Saarbrücken) I successfully applied for a tandem research project (2 full PhD positions) in the DFG SPP 1506 "Transport processes at fluidic interfaces", which after an initial 3 year funding period was extended for another 3 years.

## — Theses Reviews & Mentoring

- Fabian Mönkeberg, "Asymptotic and Numerical Methods for the Two-Dimensional Narrow Escape Problem for Finite-Size Particles", Master Thesis (with B. Wagner), Department of Mathematics, Technische Universität Berlin (2015).
- Sebastian Jachalski, "Derivation and Analysis of Lubrication Models for Two-Layer Thin-Films", Ph. D. Thesis, (with B. Wagner and B. Niethammer), Department of Mathematics, Technische Universität Berlin (2014).

## — Selected Presentations (Invited & Organized)

- "The Stokes flow and thin films with contact lines", Univ. Heidelberg (2018, invited).
- "Motion of thin droplets over surfaces", ICERM Workshop (2017, Providence, USA, invited).
- "Variational structure of fluid motion with contact lines in thin-film models", Universität der Bundeswehr, (2017, München, invited).

# CURRICULUM VITAE: DR. DIRK PESCHKA

---

- "Modelling and simulation of suspension flow", Univ. Bonn (2017, invited).
- "Towards the optimization of Ge micro-bridges", The 19th European Conference on Mathematics for Industry, (2016, Santiago de Compostela, organized).
- "Thin film free boundary problems—Modelling of contact line dynamics with gradient formulations", CeNoS-Colloquium (2016, Münster, invited).
- "Modelling and applications of bilayer flows", Seminar of the GRK 1276 "Structure Formation and Transport in Complex Systems", (2015, Saarbrücken, invited).
- "Droplets on liquids and their long way into equilibrium", 8th International Congress on Industrial and Applied Mathematics (ICIAM) (2015, Beijing, CHN, organized).
- "Numerics of contact line motion for thin films", MATHMOD 2015, Minisymposium Free Boundary Problems in Applications (2015, Wien, organized).
- "Thin-film equations with free boundaries", Jahrestagung der Deutschen Mathematiker-Vereinigung (DMV), Minisymposium Mathematics of Fluid Interfaces (2015, Hamburg, invited).
- "Liquid/liquid dewetting—Theory and experiments", Workshop Thin Liquid Films and Fluid Interfaces: Models, Experiments and Applications (2012, Banff, CAN, invited).
- "Liquid/liquid dewetting-stationary solutions", Max-Planck-Institut für Mathematik in den Naturwissenschaften, AG Musterbildung (2011, Leipzig, invited).
- "Stationary solutions in liquid/liquid dewetting", University of California Los Angeles, Department of Mathematics, Applied Math. Colloquium, (2011, Los Angeles, USA, invited).
- "Self-similar rupture for thin films with slip", EUROMECH Colloquium 497—Recent Developments and New Directions in Thin-Film Flow (2009, Edinburgh, UK, invited).

The complete list is available at <https://www.wias-berlin.de/people/peschka/>.

## — Minisymposium Organization

- "Multiple scales in electromagnetic devices - from quantum mechanical effects to circuit simulation" at The 20th European Conference on Mathematics for Industry (2018, Budapest) organized jointly with N. Rotundo, P. Farrell (WIAS, TUHH).
- "Mathematical methods for semiconductors" at the 7th European Congress of Mathematics (ECM) (2016, Berlin) organized jointly with N. Rotundo and P. Farrell (WIAS, TUHH).
- "Charge transport in semiconductor materials: Emerging and established mathematical topics" at The 19th European Conference on Mathematics for Industry (2016, Santiago de Compostela) organized jointly with N. Rotundo and P. Farrell (WIAS, TUHH).
- "Free Boundary Problems in Applications: Recent Advances in Modelling, Simulation and Optimization" at the MATHMOD (2015, Wien) organized jointly with S.J. Kimmerle (Uni BW München).
- "Recent Progress in Modelling and Simulation of Multiphase Thin-film Type Problems" at the 8th International Congress on Industrial and Applied Mathematics (2015, Beijing, CHN) organized jointly with L. Wang (Univ. Minnesota).
- "Coupled flows and their robust discretisation" at CMAM-5 2012 (Berlin) organized jointly with A. Linke (WIAS).

## LIST OF PUBLICATIONS: DR. DIRK PESCHKA

---

### — Publications

- [P1] D. Peschka, S. Bommer, S. Jachalski, R. Seemann, and B. Wagner. Impact of energy dissipation on interface shapes and on rates for dewetting from liquid substrates. *Scientific Reports*, 8(1):13295, 2018.
- [P2] D. Peschka. Variational approach to contact line dynamics for thin films. *Physics of Fluids*, 30(8):082115, 2018.
- [P3] A. Mielke, D. Peschka, N. Rotundo, and M. Thomas. On Some Extension of Energy-Drift-Diffusion Models: Gradient Structure for Optoelectronic Models of Semiconductors. In *European Consortium for Mathematics in Industry*, volume 26, pages 291–298. Springer, 2016.
- [P4] D. Peschka. Thin-film free boundary problems for partial wetting. *Journal of Computational Physics*, 295:770–778, 2015.
- [P5] R. Huth, S. Jachalski, G. Kitavtsev, and D. Peschka. Gradient flow perspective on thin-film bilayer flows. *Journal of Engineering Mathematics*, 94(1):43–61, 2015.
- [P6] S. Jachalski, D. Peschka, A. Münch, and B. Wagner. Impact of interfacial slip on the stability of liquid two-layer polymer films. *Journal of Engineering Mathematics*, 86(1):9–29, 2014.
- [P7] N. Murisic, B. Pausader, D. Peschka, and A.L. Bertozzi. Dynamics of particle settling and re-suspension in viscous liquid films. *Journal of Fluid Mechanics*, 717:203–231, 2013.
- [P8] S. Jachalski, R. Huth, G. Kitavtsev, D. Peschka, and B. Wagner. Stationary solutions of liquid two-layer thin-film models. *SIAM Journal on Applied Mathematics*, 73(3):1183–1202, 2013.
- [P9] S. Bommer, F. Cartellier, S. Jachalski, D. Peschka, R. Seemann, and B. Wagner. Droplets on liquids and their journey into equilibrium. *The European Physical Journal E*, 36(8):87, 2013.
- [P10] D. Peschka, A. Münch, and B. Niethammer. Self-similar rupture of viscous thin films in the strong-slip regime. *Nonlinearity*, 23(2):409, 2010.

## **Arbeitgebererklärung**

Die aufnehmende Einrichtung

Weierstraß-Institut für Angewandte Analysis und  
Stochastik (WIAS),  
Leibniz-Institut im Forschungsverbund Berlin e. V.

stellt Herrn

Dr. Dirk Peschka

im Falle der Bewilligung seines Antrags auf die Eigene Stelle durch die Deutsche Forschungsgemeinschaft (DFG) befristet für die Dauer seiner Förderung mit der Eigenen Stelle als wissenschaftlichen Mitarbeiter ein. Sie stellt ihm für diesen Zeitraum die notwendige Grundausstattung (z.B. Laborräume, Büroräume etc.) zur Verfügung. Es gelten die an der Einrichtung einschlägigen Tarifvorschriften mit der Maßgabe, dass

a) sich die Arbeitspflicht von Herrn Dr. Dirk Peschka

auf sein von der DFG gefördertes Forschungsvorhaben

Mathematical modeling and simulation of substrate-flow interaction using generalized gradient flows

und damit unmittelbar zusammenhängende wissenschaftliche Dienstleistungen beschränkt und

b) der Arbeitgeber nicht durch dienstliche Anordnungen Einfluss auf die selbständige Bearbeitung des genannten Forschungsvorhabens nimmt.

Der Unterzeichnende bestätigt, dass die für die Unterzeichnung notwendige Befugnis vorliegt und alle notwendigen internen Abstimmungen erfolgt sind.

Berlin, 12.10.2018



Prof. Dr. Michael Hintermüller, Direktor des WIAS

Cite this: DOI: 10.1039/xxxxxxxxxx

## Signatures of slip in dewetting polymer films<sup>†</sup>

Dirk Peschka,<sup>a</sup> Sabrina Haefner,<sup>b</sup> Karin Jacobs,<sup>b</sup> Andreas Münch,<sup>c</sup> Barbara Wagner<sup>a</sup>Received Date  
Accepted Date

DOI: 10.1039/xxxxxxxxxx

www.rsc.org/journalname

Thin liquid polymer films on hydrophobic substrates are susceptible to rupture and formation of holes, which in turn initiate a complex dewetting process that ultimately evolves into characteristic stationary droplet patterns. Experimental and theoretical studies suggest that the specific type of droplet pattern largely depends on the nature of the polymer-substrate boundary condition. To follow the morphological evolution numerically over long time scales and to resolve the multiple length scales involved has so far been a major challenge. In this study a highly adaptive finite-element based numerical scheme is presented that allows for large-scale simulations to follow the evolution of the dewetting process deep into the nonlinear regime of the model equations, capturing the complex dynamics including shedding of droplets. In addition, the numerical results predict the previously unknown shedding of satellite droplets during the destabilisation of liquid ridges, that form during the late stages of the dewetting process. While the formation of satellite droplets is well-known in the context of elongating fluid filaments and jets, we show here that for dewetting liquid ridges this property can be dramatically altered by the interfacial condition between polymer and substrate, namely slip. This work shows how in general interface properties can be systematically used to influence pattern formation processes.

### 1 Introduction

In fluid mechanics, the no-slip condition is widely accepted as the appropriate boundary condition for flows of Newtonian liquids sheared along a solid surface. A notable exception arises in the presence of a moving contact line between a liquid and the solid substrate, where the use of the no-slip condition leads to a singularity in the stress field<sup>2,3</sup>. In the past decades, however, it has been shown that thin films of polymer melts can exhibit significant slip when sheared along a substrate, where slip lengths much larger than the film thickness have been observed<sup>4–10</sup>.

For retracting rims, as they emerge after a hole or trench has opened, the magnitude of slip has a direct impact on its shape and dynamics. When slip is very small or zero, the retraction rate is independent of the size of the growing rim and hence approximately constant, except for logarithmic corrections<sup>11</sup>. For slip that is large compared to the film thickness, viscous dissipation increases with the rim size and this gives rise to a  $t^{-1/3}$  power law in time  $t$  for the retraction (dewetting) rate<sup>12</sup>, and has been confirmed experimentally<sup>13–16</sup>. In both cases, the moving rim is susceptible to span-wise instabilities<sup>17–19</sup>, but for the case where slip is large compared to the film thickness, the dependence of the

retraction velocity on the local rim size provides a crucial amplifying mechanism for the instability, which is absent in the no-slip situation<sup>20</sup>. As a consequence, the repeated shedding of droplets during dewetting leaves a characteristic pattern, that is absent for systems with no-slip. In either case, the dewetting rims eventually meet to form residual ridges, which in either case are susceptible to a Rayleigh-Plateau type instability with almost the same dominant wave-length<sup>21</sup>. Eventually, this leads to the break-up into droplets. As a result of this long-time process, a strikingly different droplet patterns is obtained, as shown in experiments, see Fig. 1.

The evolution of the polymer melts during these dewetting regimes, from early dewetting stages after hole formation to the late stages of rupture of the ridges, where the hole boundaries meet, is most conveniently modelled by thin-film models. A systematic asymptotic derivation from full Navier-Stokes equations<sup>22,23</sup>, exploiting the separation between the lateral and normal length, revealed that the resulting dimension-reduced thin-film model depends on the order of magnitude of slip, leading to two asymptotic distinguished limits: a weak-slip and a strong-slip regime, with important limits given by the no-slip and intermediate-slip cases.

While thin-film models have been shown to be of great advantage for the analysis of free boundary problems, predicting the evolution over long time and large spatial scales deep into the nonlinear regimes is still an extremely difficult task. A major problem is to resolve the length scales associated with nanoscopic

<sup>a</sup> Weierstrass Institute for Applied Analysis and Stochastics, Mohrenstr. 39, 10117 Berlin, Germany. E-mail: dirk.peschka@wias-berlin.de

<sup>b</sup> FR 7.2 Experimentalphysik, Saarland University, 66041 Saarbrücken, Germany.

<sup>c</sup> Mathematical Institute, University of Oxford, Andrew Wiles Building, Oxford OX2 6GG, UK.

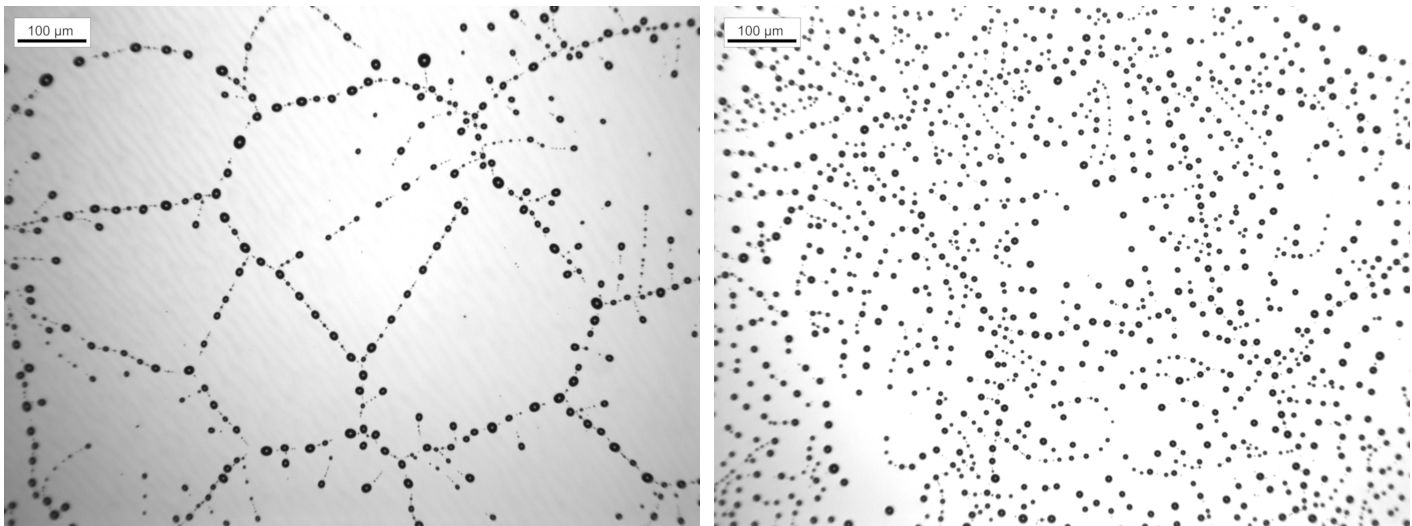


**Fig. 1** Stationary droplet pattern of a 110 nm thick polystyrene PS(10.3k) film after dewetting at  $T = 120^\circ\text{C}$  from a hydrophobically coated Si wafer: (**left**) AF 1600 and (**right**) DTS coating (Images: Courtesy of L. Marquant<sup>1</sup>)

residual layers that remain after the film has dewetted, typically about  $\sim 0.1 - 1\text{ nm}$ , up to thickness of about  $\sim 10 - 1000\text{ nm}$  of the growing rim, and to account for the slip length in the range of  $1 - 1000\text{ nm}$ , and the length scale of the resulting instability  $10^3 - 10^4\text{ nm}$ . By far the greatest challenge is to make predictions regarding phenomena on the length scales of the instabilities, while using numerical solutions with a fine spatial resolution on the length scale of the residual layer.

In this article we present a numerical algorithm that is able to answer this need featuring a strategy for local adaptivity and an optimized treatment of the intermolecular potential. We will show that the difference in slip lengths indeed leads to the instability patterns seen in experiments. Our numerical solutions also confirm the Rayleigh-Plateau type instability of the residual ridges during the late phases of the dewetting for both cases, the no-slip and the intermediate-slip cases, with similar wave-lengths at the onset, which had been predicted previously based on a linear stability analysis<sup>18,21</sup>. Similar studies were concerned with cases of infinite ridges with<sup>24</sup> and without<sup>25</sup> gravity, followed by a broad range of investigations in the literature for this situation using different contact line models and approximations. Numerically, the work by Diez et al.<sup>26</sup> focuses on finite length ridges but also includes a review and elucidating comparison of results for the infinite case. Here, most unstable modes are due to varicose perturbations, and the preferred wave-length of the instability is set by the balance of the destabilising capillary forces, contact-line conditions, and, for sufficiently viscous liquids, by the viscous dissipation. Stability analysis of the effect of slip vs. no-slip on the instability of a stationary ridge show that both are linearly unstable and have similar wave-lengths<sup>18,21</sup>.

Our numerical methods allow to follow the evolution until rupture and show significant morphological differences. In particular, they reveal that while for the no-slip case the break-up is accompanied by the formation of a cascade of satellite droplets, that has never been seen before in this context. Moreover, for the intermediate-slip case they disappear.

In other contexts such as liquid jets or fluid filaments, satellite droplets during rupture are well-known, see e.g. the work by Tjahjadi et al.<sup>27</sup> or the review by Eggers and Villermiaux<sup>28</sup>. Here, we show for the first time that while the self-repeating rupture of satellite droplets is established for the no-slip boundary condition of a rupturing ridge, they disappear for the intermediate-slip condition. Interestingly, a closer look at experimental results validates these predictions.

In the following sections we first introduce the underlying model equations governing the long-time dewetting process. We revisit analytical results on dewetting rates and their connection to the destabilisation of the rim during the early stages of the dewetting film in section 2. We compare the predictions to experimental results in section 2.3.

To capture the morphological details well-into the nonlinear regime including droplet pin-off scenarios, observed in experiments, we introduce in section 3 a highly adaptive numerical method necessary to bridge the multiple length scales over long time regimes. In section 4 we address the late scenario when the rims of the holes meet and eventually disintegrate into droplets, where we predict a new scenario of cascades of satellite droplets for the no-slip case.

## 2 Thin-film models and instability

### 2.1 Problem formulation

Once the film has ruptured by nucleation or by external forcing, forming a hole, or, in a planar-symmetric setting, a trench, the viscous fluid retracts to reduce the overall energy of the liquid-gas, solid-liquid and solid-gas interfaces. The dewetting process is driven by the intermolecular potential  $\phi$  between the film and the substrate, that is given, in the simplest case, by the attractive long-range van-der-Waals forces and short-range Born repulsion forces, the minimum of which yields the height  $h_*$  that is left behind after the film has dewetted. Motivated by Lennard-Jones potentials, one often finds intermolecular potentials<sup>29,30</sup> of the

standard form  $\phi(h) = \tilde{\phi}(h/h_*)$ , where

$$\tilde{\phi}(h) = \frac{(-S)}{n-m} (nh^{-m} - mh^{-n}), \quad (1)$$

with  $m = 2, n = 8$ ,  $\phi'(h_*) = 0$  and  $\phi(h_*) = -S$ . For partial wetting the spreading coefficient is negative and hence  $S < 0$ .

Due to the slow dewetting rates of the polymer films with chain lengths below the entanglement lengths, the Navier-Stokes equations serve as the underlying model for the viscous fluid but with an effective slip boundary condition at the substrate. The scale separation of the characteristic length scale  $H$  normal and the length scales  $L$  tangential to the substrate allow a consistent thin-film approximation in the small parameter  $\varepsilon \approx H/L \ll 1$  that leads to the reduction of the free-boundary problem to a problem for the free boundary  $h$  in closed form. We assume that the time-dependent domain  $\Omega(t) \subset \mathbb{R}^3$  occupied by the viscous fluid can be parametrized using a nonnegative scalar function  $h : [0, T] \times \bar{\Omega} \rightarrow [0, \infty)$  such that

$$\Omega(t) = \{(\mathbf{x}, z) : \mathbf{x} \in \bar{\Omega}, 0 < z < h(t, \mathbf{x})\}, \quad (2)$$

where the film height  $h(t, \mathbf{x})$  depends on time  $t \in [0, T]$  and on space  $\mathbf{x} = (x, y) \in \bar{\Omega} \subset \mathbb{R}^2$  with given initial data  $h_0(\mathbf{x}) = h(t=0, \mathbf{x})$  (see Fig. 2). It has been shown that depending on the magnitude of (effective) slip length there exist two asymptotic distinguished limits<sup>22</sup>, leading to the weak-slip thin-film model, given by the fourth-order parabolic partial differential equation (PDE)

$$\partial_t h - \nabla \cdot (m(h) \nabla \pi) = 0. \quad (3a)$$

where the mobility is

$$m(h) = h^3 + bh^2 \quad (3b)$$

and the generalized pressure  $\pi$  is defined as the functional derivative of the energy functional

$$E(h) = \int_{\bar{\Omega}} \frac{1}{2} |\nabla h|^2 + \phi(h) \, d\mathbf{x}, \quad (3c)$$

with respect to  $h$ , that is,

$$\pi = \frac{\delta E}{\delta h} = -\nabla^2 h + \Pi(h), \quad (3d)$$

and  $\Pi(h) = \partial_h \phi(h)$  is the derivative of the intermolecular potential.

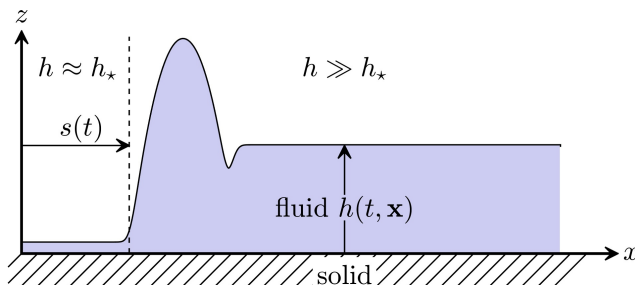


**Fig. 2** Sketch of solution  $h(t, \mathbf{x})$  in the  $x-z$  plane.

The second distinguished limit leads to the strong-slip thin-film

model given by the system of partial differential equations for  $h$  and the lateral velocity  $\mathbf{u} = (u, v)$  with components  $u$  and  $v$  in the  $x$  and  $y$ -direction, respectively

$$\text{Re} (\partial_t \mathbf{u} + (\mathbf{u} \cdot \nabla) \mathbf{u}) = \frac{1}{h} \nabla \cdot \boldsymbol{\sigma} - \nabla \pi - \beta^{-1} \frac{\mathbf{u}}{h} \quad (4a)$$

$$\partial_t h + \nabla \cdot (h \mathbf{u}) = 0, \quad (4b)$$

where  $\text{Re}$  is the Reynolds number and  $\beta$  is related to the slip length  $b$  via  $b = \beta/\varepsilon^2$  and the effective shear stress is

$$\boldsymbol{\sigma} = h [\nabla \mathbf{u} + (\nabla \mathbf{u})^\top + 2(\nabla \cdot \mathbf{u}) \mathbb{I}]. \quad (4c)$$

The important limiting cases are the well-known no-slip model, where the degenerate mobility is  $m(h) = h^3$  and the so-called intermediate-slip model, that is sometimes also referred to as the full-slip model, with the degenerate mobility  $m(h) = h^2$ . The details of the dynamic and morphological evolution strongly depend on the magnitude of slip at the solid-liquid interface as has been shown in the literature<sup>31</sup>. For no-slip or weak-slip the liquid accumulates in a growing rim in front of the contact-line, and destabilizes. The case of strong-slip is characterised by very asymmetric retracting rim solutions with a monotone spatial decay towards the unperturbed film for particularly large slip, that undergoes a transition to oscillatory decay for as the slip length decreases below a critical value<sup>22,32</sup>. This observation has been used to identify the strong slip regime in experiments and in fact also to determine the amount of slip quantitatively<sup>33–35</sup>, and investigate the molecular causes of slip in polymer melts<sup>36</sup>. An overview about this topic can be found in the work by Bäumchen and Jacobs<sup>37</sup>.

## 2.2 Dewetting rates

We first discuss the dynamics of the cross section of an unperturbed rim, i.e. where  $\partial_x h = 0$ . In the case of no-slip,  $m(h) = h^3$ , the evolution is determined by the region near the effective contact line where the rim meets the residual film of thickness of about  $h = h_*$  that is left behind the dewetting front. A careful asymptotic analysis and comparison with long-time numerical solutions<sup>22,38</sup> reveals that the dewetting rate is nearly constant and in fact the position of the contact line  $s(t)$  is, to leading order, given by the nearly linear law

$$s(t) \sim \frac{t \tan^3(\theta)}{\ln(3(h_\infty/h_*)t)} \quad (5)$$

as  $t \rightarrow \infty$ , where  $h_\infty = \lim_{x \rightarrow \infty} h$ . Physically, this reflects the fact that the size of the rim only has a weak effect on the total friction and hence in turn on the dewetting velocity.

For intermediate slip, where  $m(h) = h^2$ , the evolution of the unperturbed rim is different. At any given size, the rim behaves like a traveling wave, but with a wave speed that depends on the size of the rim, which by mass conservation is proportional to the distance travelled. A detailed asymptotic analysis<sup>22,38</sup> that matches the rim to the unperturbed and the residual film gives

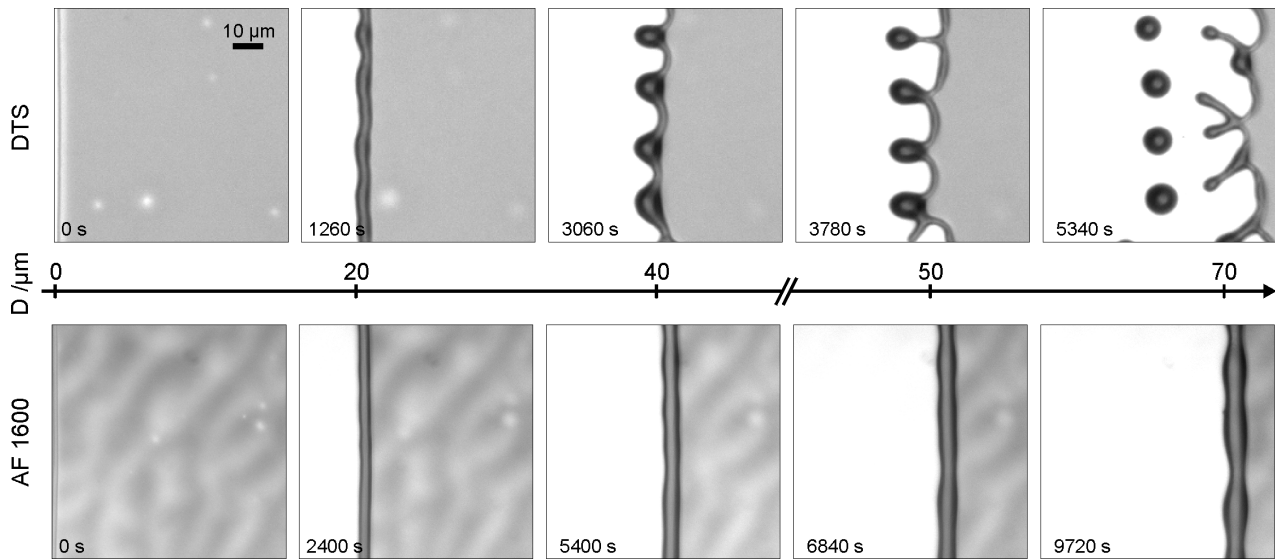


**Fig. 3** Series of micrographs characteristic for experiments for films exposed to intermediate (**upper row**, dewetting off hydrophobized Si wafer covered with a silane monolayer DTS) and to no-slip (**lower row**, dewetting off AF 1600-covered Si-wafer). In both series, a 100 nm thin PS(13.7k) film dewets at  $T = 120^\circ\text{C}$ . In both series, undulations are formed along the rim, however, only in the intermediate slip case above budding is observed that later leads to fingers and a pinch-off of droplets. Comparing rims that have travelled a similar distance ensures that only rims of similar volumes are evaluated.

the leading order result

$$s(t) \sim \left( \frac{9Mb \tan^5 \theta}{4h_\infty} \right)^{1/3} t^{2/3}. \quad (6)$$

in the limit  $t \rightarrow \infty$ , where  $b$  is the slip length and  $M \approx 0.0272$ . A similar prediction had been made by Reiter and Khanna<sup>13</sup>.

Rims with capillary humps like the ones that appear here are known to be subject to Rayleigh-Plateau like instabilities<sup>21,24,26</sup>, where the higher capillary pressure in thinner parts squeezes even more liquid into the thicker parts, hence promoting the growth of undulations along the rim. The linear stability of dewetting rims is complicated by the fact that the base state itself grows in time, giving rise to a linearised PDE that cannot be solved exactly using separation of variables. Instead, the linearised PDE can be solved numerically, and the amplification of an initial perturbation tracked in time<sup>40</sup>. Interestingly, the perturbation evolves into a universal long-time shape that is not sensitive to the initial perturbation. Comparing these shapes reveals an important difference between the no-slip and the intermediate slip case: The former is much more symmetric and closer to the classical varicose mode observed in the Rayleigh-Plateau instability than the latter. Moreover, the maximum amplification was significantly higher for the intermediate slip case.

These results were analysed further using an asymptotic sharp-interface approach for large rims and a WKB analysis, which established that the long-time dominant wave-number is given by an equal area rule and is shorter than predicted by a frozen-mode analysis<sup>41,42</sup>. Direct numerical simulations of the nonlinear PDE with perturbed rims as initial data confirm that indeed, the intermediate slip is much more unstable than the no-slip case, and perturbations grow asymmetrically<sup>21</sup>, as shown in Fig. 8. It is clearly seen that the perturbations in the rim for the no-slip case remain small, while in the intermediate-slip case, they grow, giving

rise to fingers that eventually pinch-off and then the process repeats itself. This is seen also in experimental data in Fig. 3. The physical explanation for these different manifestations relates to the size-dependence of the friction. In the intermediate slip case, thicker parts of a perturbed rim have a smaller velocity than thinner ones and tend to lag further behind. This supplies an additional instability mechanism that reinforces the Rayleigh-Plateau instability, but is essentially absent in the no-slip case where the dewetting rate is largely independent of the rim size<sup>19,40,42</sup>.

The size dependence also adds another instability mechanism by causing thicker parts of the rim to lag behind thinner parts, thus reinforcing the Rayleigh-Plateau instability and making it more asymmetric<sup>19</sup>. A linear stability analysis of the thin-film model predicts the instability to thus be much more pronounced in the intermediate-slip than in the no-slip case<sup>40–42</sup>.

For slip lengths that are much larger than the film height, the dynamics of the evolution changes yet again. In the strong slip regime, the fluid flow is plug-flow and the evolution is described by a system of PDEs for the film height and for the plug velocity, where the contribution from elongational stresses enters to the same order as the effects from the friction due to slip. Dewetting rim solutions of this model were explored numerically and asymptotically<sup>22,32</sup>. In this regime, the shape of the profile becomes highly asymmetric, with a steep side facing the dewetted area and a much flatter decay to the unperturbed film. This is well reflected in the experimental data for melts with larger polymer chains, where slip is expected to be larger. Interestingly, the change in the balance of stresses leads to an approximately linear dewetting law,

$$s(t) \sim \frac{b^{1/2} \tan^2(\theta) t}{4\sqrt{2} h_\infty^{1/2} \ln^{1/2} t} \quad (7)$$

that is, another case with an approximately constant velocity of the retracting rim, just as in the no-slip case. This suggests that

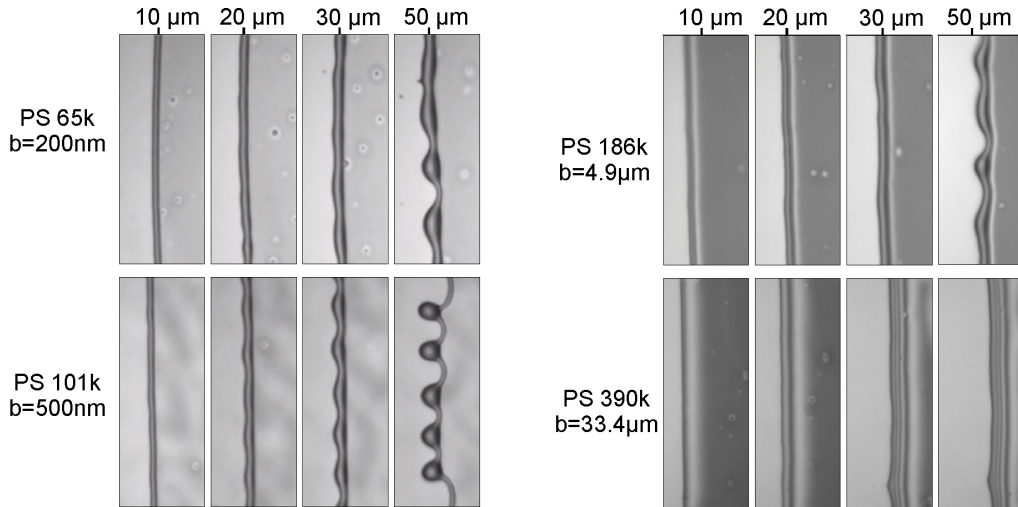


**Fig. 4** Comparisons of the dewetting behaviors of 110 nm thick PS films for different chain lengths, dewetting from AF1600 after the rim travelled the distance  $D$  given above the images. Films have been annealed to different temperatures to speed up dewetting in case of films with larger viscosities: PS(65k) at  $T = 140^\circ\text{C}$ , PS(101k) at  $T = 140^\circ\text{C}$ , PS(186k) at  $T = 150^\circ\text{C}$ , PS(390k) at  $T = 150^\circ\text{C}$ . In the chosen systems, the slip length increases with increasing molecular weight, leading to  $B = b/h$  of 1.81, 4.6, 45 and 300, respectively. The slip lengths are obtained by fitting the rim profile as reported by Bäumchen et al.<sup>36</sup> or McGraw et al.<sup>39</sup>. Clearly, fingering is suppressed for stronger slip in this system.

for very large slip lengths, the rim should become stable again.

### 2.3 Experimental set-up and methods

For the experiments, atactic polystyrene (PS, purchased from PSS, Mainz, Germany, molecular weights as listed in the experiments) is used as a model viscous liquid. The films were produced by spin-casting a toluene solution (Selectipur or LiChrosolv, Merck, Darmstadt) of PS on freshly cleaved mica sheets. The glassy thin-films were then floated onto an ultrapure water (organic impurities < 6 ppb, resistance at  $25^\circ\text{C}$ : < 18.2 M $\Omega$ cm) surface and were then picked up with hydrophobic Si wafers.

Hydrophobic Si wafers were achieved by two different preparation methods: i) on the cleaned Si surface, a self assembled monolayer (SAM) of silane molecules (dodecyltrichlorosilane, DTS, Sigma Aldrich/Merck) was prepared<sup>43</sup>, or ii) the cleaned Si wafer was dipped into a solution of a fluoropolymer layer (AF1600, Sigma Aldrich/Merck, Darmstadt, Germany).

Dewetting can be initiated by the glassy polymer film above its glass transition temperature. The dewetting of the retracting straight fronts was monitored *in situ* by optical microscopy on a heating plate (Linkam) or by atomic force microscopy (AFM, Dimension ICON, Bruker).

The dewetted distance was typically obtained from optical micrographs. In AFM experiments, the dewetted distance can also be calculated from three-dimensional scans of the rim on the basis of volume preservation. The values resulting from both approaches were checked for consistency.

Slip lengths have been calculated using the rim profile analysis method<sup>44,45</sup>; structural details, surface roughness values, and wetting properties of the coatings are given in the Supplementary Material to Ref.<sup>31</sup>. Polymer film thicknesses have been determined by ellipsometry on the glassy film or by AFM on the edge of a film.

The experimental results show in Fig. 4 support the prediction of the linear law (7), that for the strong-slip case the instability is suppressed, see the results for the largest slip length in the lower right figure for PS 390k in Fig. 4.

## 3 Numerical methods

### 3.1 Finite element solution

We now explain the intricacies of numerically resolving the multiple length scales of the problem. We focus on the two cases of no-slip and intermediate-slip as most of the experimental results regarding the various instabilities fall into either of these two regimes.

Our solution of the thin-film model (3) is based on a  $P_2$  finite element method (FEM), where the fourth-order equation is split into a system of two second-order equations. The FEM uses piecewise quadratic elements and local mesh refinement. We employ a semi-implicit time-discretization, where only the highest order derivative is treated implicitly. Therefore, the thin-film equation (3) is multiplied with a test-function  $v$  and integrated by parts and to obtain

$$\int_{\bar{\Omega}} \partial_t h v + m(h) \nabla \pi \cdot \nabla v \, d\mathbf{x} = 0, \quad (8a)$$

where boundary terms vanish due to the no-flux boundary condition  $\mathbf{n} \cdot \nabla \pi = 0$  imposed on  $\partial \bar{\Omega}$ . We also rewrite the pressure  $\pi$  in the weak form as

$$\int_{\bar{\Omega}} \pi v \, d\mathbf{x} = \int_{\bar{\Omega}} \nabla h \cdot \nabla v + \Pi(h) v \, d\mathbf{x}, \quad (8b)$$

where again we used integration by parts and  $\mathbf{n} \cdot \nabla h = 0$  on the boundary  $\partial \bar{\Omega}$ . In particular this statement of the PDE implies conservation of volume

$$\frac{d}{dt} \int_{\bar{\Omega}} h(t, \mathbf{x}) \, d\mathbf{x} = 0,$$

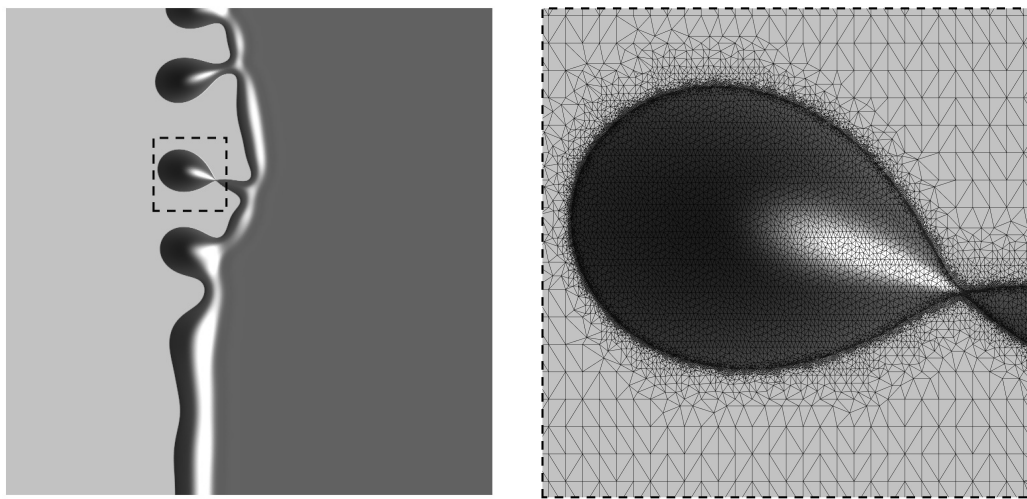


**Fig. 5** (left) Dewetting rim during pinch-off of a single droplet highlighted with dashed lines and (right) magnification of this droplet and corresponding locally refined triangulation. The mesh consists of 92272 vertices, which requires to solve for  $2 \times 368423 = 736846$  unknowns ( $h_n, \pi$ ) for the  $P_2$  FEM discretization at each time-step.

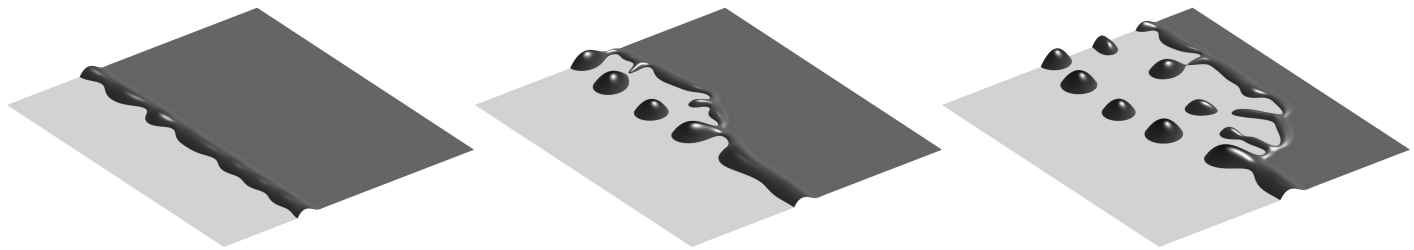


**Fig. 6** Simulated pattern formation: 3D view with light shaded areas showing dry regions, whereas elevated darker areas indicate the liquid/air interface.

which can be seen when selecting  $v = 1$  in the continuous or the discrete weak formulation. Evaluating the solution at discrete times  $h_n(\mathbf{x}) = h(n\tau, \mathbf{x})$  we use the time-discretization  $\partial_t h = \tau^{-1}(h_n - h_{n-1})$ . This allows us to rewrite the weak form of the thin-film model in (8) so that we seek  $(h_n, \pi) \in W$  such that

$$\int_{\bar{\Omega}} h_n v + \tau m^* \nabla \pi \cdot \nabla v \, d\mathbf{x} = \int_{\bar{\Omega}} h_{n-1} v \, d\mathbf{x}, \quad (9a)$$

$$\int_{\bar{\Omega}} \pi w - \nabla h_n \cdot \nabla w \, d\mathbf{x} = \int_{\bar{\Omega}} \Pi^* w \, d\mathbf{x}, \quad (9b)$$

which needs to hold for all  $(v, w)$  from a suitable function space  $W$ . When we define  $m^* = m(h_{n-1})$  and  $\Pi^* = \Pi(h_{n-1})$  this becomes a semi-implicit time-discretization. The FEM constitutes a method for the construction of a finite-dimensional subspace  $W_h \subset W$ , where we have an admissible decomposition  $\bar{\Omega} = \bigcup_{k=1}^N \mathcal{T}_k$  of the domain into triangles  $\mathcal{T}_k$ , on which we define  $W_h$  as the space of continuous functions which are piecewise quadratic on each triangle, *i.e.*  $P_2$  finite elements. Then we seek a discrete solution  $(h_n, \pi) \in W_h$  of (9) valid for all  $(v, w) \in W_h$ . The integrals appearing in (9) are solved exactly or using 7-point Gauss quadrature. A typical droplet pattern emerging from the simulation with  $m = h^2$  is shown in Fig. 6.

The main difficulties in solving (9) are due to the fact that one needs to choose the  $h_*$  contained in  $\Pi(h)$  quite small. Then the solution  $h$  will feature large regions where the solution is either almost constant  $h \approx h_*$  or the solution is smooth and  $h \gg h_*$ , as

shown in Fig. 2. However, where those regions meet the solution features a kink which should be resolved in the triangulation, cf. Fig. 5. We perform a heuristic local mesh refinement in these connecting regions, where the contact line is situated. Assuming the solution does not change drastically in time and having a finer mesh also in the neighborhood of this kink allows us to keep a locally refined mesh a number of discrete time-steps. When constructing a new mesh, we start from a coarse base mesh and determine which of its elements are crossed by the contact line

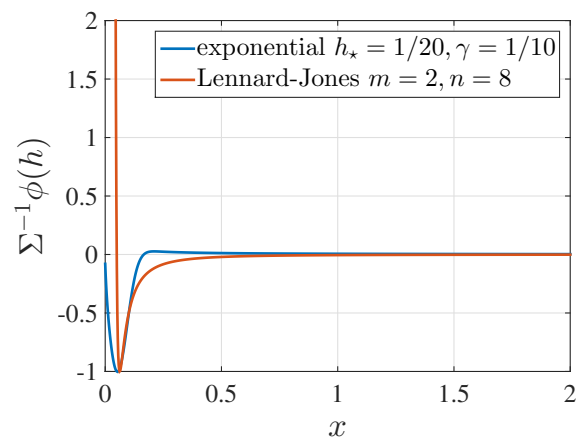


**Fig. 7** Lennard-Jones potential (1) compared to the much more short-ranged exponential potential (10) both with  $h_* = 1/20$ ,  $\epsilon_* = 1/16$ .

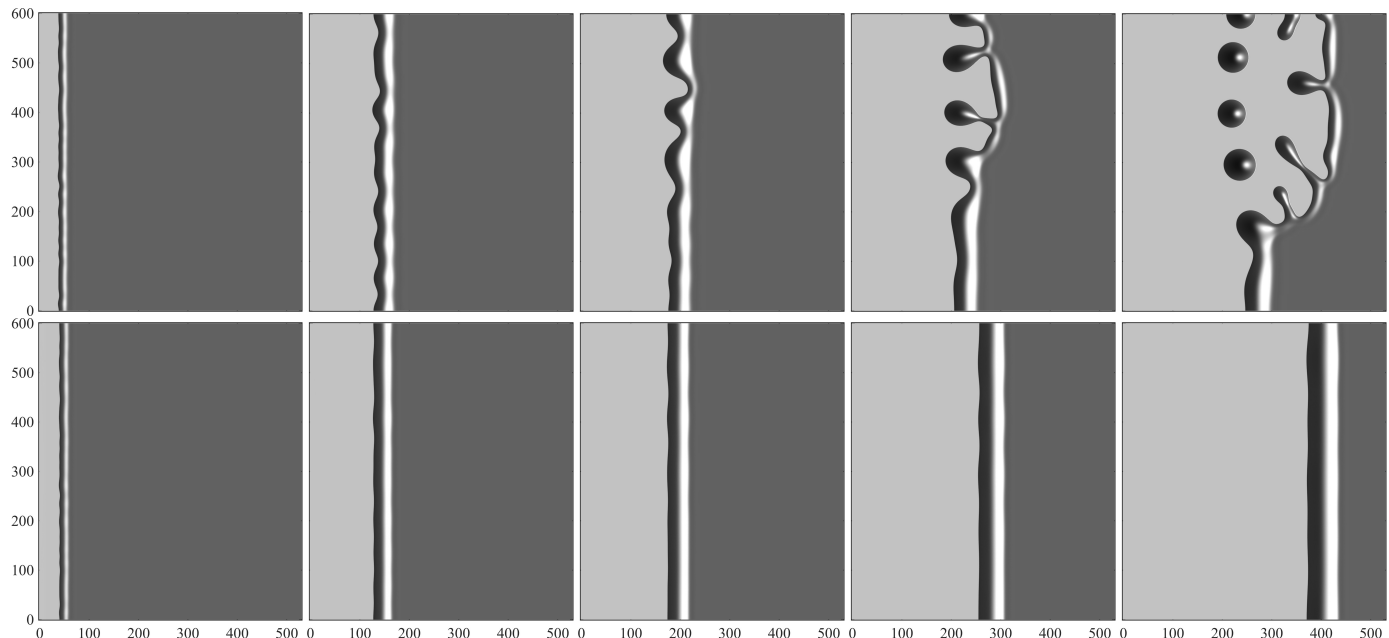


**Fig. 8** Numerical solutions for (**upper**) mobility  $m = h^2$  and (**lower**) mobility  $m = h^3$  with initially straight front with random oscillating perturbation and time progressing from left to right (shown for similar rim progression)

of the previous solution. Those elements are refined by inserting additional vertices to an extend, that the kink is resolved again. Furthermore we make sure that also neighboring elements are refined. Based on the set of newly created vertices we perform a new triangulation and interpolate the old solution onto the new triangulation.

In order to allow the control of the minimum and the derivatives of  $\phi$  separately via  $h_*$  and  $\varepsilon_*$  it is advantageous to work with an alternative potential representation  $\phi(h) = \widehat{\phi}((h - h_*)/\varepsilon_*)$  with

$$\widehat{\phi}(s) = -\Sigma \left( \frac{\gamma}{1+s} - (1+\gamma) \exp(-s^2) \right), \quad (10)$$

which has similar properties as (1). In particular, with this potential we still have the same  $\Gamma$ -convergence property as  $h_*, \varepsilon_* \rightarrow 0$ . This abstract statement ensures that equilibrium contact angles are maintained and that the energetic contribution of  $\phi$  from (10) and from (1) coincide in this limit. We note that for  $0 < \gamma \ll 1$  the minimum slightly shifts away from  $h_*$ , however, one gains a slightly stabilizing potential with  $\phi'' > 0$  for  $h \gg h_*$ . In addition we point out that we monitor that the minimum of the solution  $\min_{\mathbf{x}} h(t, \mathbf{x})$  never violates the nonnegativity requirement that  $\phi \rightarrow \infty$  as  $h \rightarrow 0$  (see Fig. 7), in particular, by keeping the time-step size  $\tau$  sufficiently small, see also previous mathematical studies<sup>46,47</sup> that incorporate the nonnegativity property into their numerical scheme.

### 3.2 Initial data for rims and ridges

We still need to specify the initial data  $h_0(\mathbf{x})$  for the numerical simulation in order to describe the various stages of the dewetting process. In experiments, the dewetting is started from a uniform flat layer bounded by a nearly straight edge. When the sample is heated the layer liquidifies and the edge becomes a moving

contact line of the dewetting process. In simulations we choose the supporting domain sufficiently large  $\bar{\Omega} = [0, L] \times [0, 600]$  with  $L \sim 500$ , and using  $h_* = 1/20$  we represent the uniform layer with the nearly straight contact line at  $x_0$  using an initial film thickness

$$h_0(\mathbf{x}) = h_* + \frac{1}{2} \left( 1 + \tanh \left[ \frac{x - x_0(y)}{\delta} \right] \right), \quad (11)$$

with the smooth initial contact line position  $x_0(y) = 20 + \sum_{n=1}^{50} a_n \cos(n\pi y/600)$ . With  $\delta = 1/2$  one can interpret  $h_0$  to be an approximation of a step-like profile, where slight corrugations of  $x_0$  along  $y$ -direction are introduced using the normally-distributed coefficients  $a_n$  with zero mean and standard deviation  $1/10$ . This choice is then maintained throughout all dewetting simulations for various mobilities.

For long times and domain size far beyond  $\bar{\Omega}$ , one can observe multiple dewetting rims colliding and forming capillary ridges. In order to study the stability of a capillary ridge, we first compute a 1D stationary solution  $h_{\text{stat}}(x)$  and the linear stability with respect to perturbations  $h(t, \mathbf{x}) = h_{\text{stat}}(x) + \delta h_1(x; k) e^{iky + \sigma t}$ , with fixed wavenumber  $k$ , which returns an eigenproblem for the perturbation  $h_1$  of the base state<sup>21,42</sup>. Then we select an unstable mode  $k$ , usually the most unstable, and use initial data of the form

$$h_0(\mathbf{x}) = h_{\text{s}}(x) + \delta h_1(x; k) \cos(ky), \quad (12)$$

with a sufficiently small  $\delta$ , so that also the non-negativity of  $h_0$  is not violated. In the linear regime we expect to see an exponential amplification of the perturbation as indicated above, however, we are interested in using the numerical simulation as a tool to observe features in the nonlinear regime which are distinctive features of the ridge shape, *e.g.*, secondary or tertiary droplets, the general form of the intermolecular potential is the same but we

use  $h_* = 1/40$ . In order to study the systematic effect of the slip boundary condition on dewetting patterns, we study the contact-line instability of moving rims and stationary ridges for the mobility function  $m(h) = h^3$  (no-slip) and  $m(h) = h^2$  (intermediate-slip). In figure 8 the evolution of the rims for no-slip and intermediate-slip is shown at times, where they have accumulated the same volume, starting with the same initial film thickness as given in the experiments. This corresponds to the experimental results where the evolution of the rims are shown at the same distance measured from the initial coordinates. For the first time the striking dewetting patterns for the intermediate-slip case is observed, while for the no-slip case only shallow oscillation will accrue, in excellent comparison with the experimental results in Fig. 3

## 4 Break-up of a liquid ridge

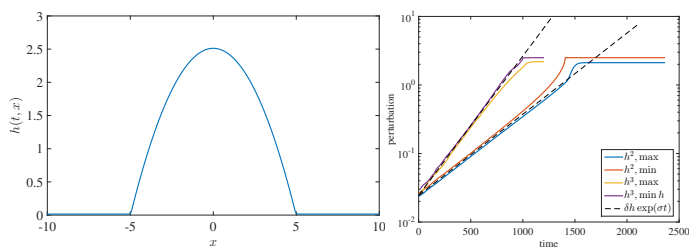


**Fig. 9 (left)** 1D steady state  $h_0$  with  $\epsilon_* = 1/20$ ,  $h_* = 1/80$  and **(right)** amplification of a perturbation (13) to the initial state showing  $\min_y h(t, x = 0, y)$  and  $\max_y h(t, x = 0, y)$  from numerical solution with  $\sigma$  compared to the prediction of linear stability<sup>21</sup>  $h - h_0 \sim \exp(\sigma t)$  for  $h^2$  and  $h^3$  mobility.

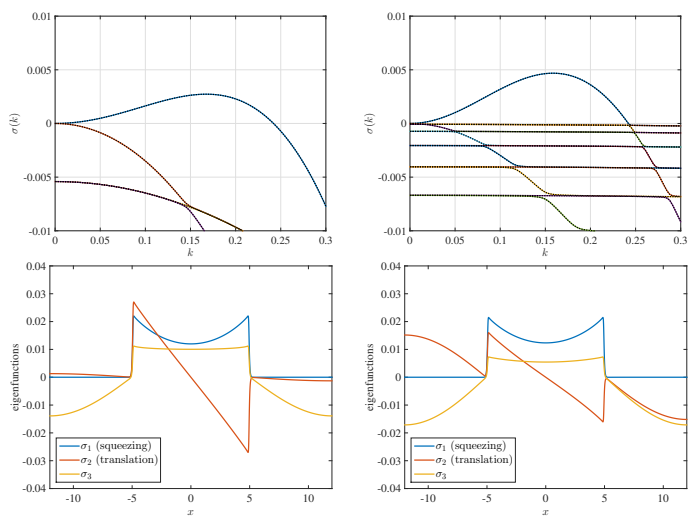


**Fig. 10** Dispersion relation  $\sigma(k)$  for **(upper left)**  $h^2$  and **(upper right)**  $h^3$  with overlapping results for exponential and standard potential (full and dotted lines), and below **(bottom)** the corresponding eigenmodes for most unstable wavenumber are shown.

Towards the final stages of dewetting process the rims approach each other and merge, yielding a polygonal network of ridges. As is known from previous studies stationary ridges are susceptible to Rayleigh-Plateau type instability for both no-slip and intermediate boundary conditions at the substrate. Both, the no-slip and the intermediate-slip case have been extensively investigated

in the literature<sup>21,24,26</sup>.

### 4.1 Comparisons with linear stability analysis

We first summarise the linear stability of a (stationary) ridge, which is carried out by King et al.<sup>21</sup> in detail. Stationary ridges appear as time-independent two-dimensional solutions of (3), that is, with  $\partial_t h \equiv 0$ ,  $\partial_y h \equiv 0$ , with a constant film thickness  $h \rightarrow h_c$  at  $x \rightarrow \pm\infty$ . An example for such a solution is shown on the left in Fig. 9, with a symmetric and approximately parabolic shape around the maximum. The defining boundary value problem invariant against translations and simultaneous rescaling of  $x$  and  $h$ , and therefore the solutions form a two parameter family, where each member is uniquely specified by the location and height of the maximum. A linear stability analysis that introduces perturbations of the form

$$h(t, x, y) = h_0 + \delta h_1(x; k) \exp(iky + \sigma t) \quad (13)$$

was carried out for (3) using asymptotic techniques. We summarise here only the salient features relevant to the comparison and discussion here.

Solving the eigenvalue problem for  $\sigma(k)$  that results from introducing (13) numerically reveals that as  $k \rightarrow 0$ , the top two eigenvalues (i.e. with the largest real part) are real and tend to zero. The larger one is associated with the scale invariance and hence corresponds to varicose perturbations of the ridge and is the only eigenvalue that is positive, hence unstable for a range of wavenumbers  $0 < k < k_c$  but stable for  $k > k_c$ .

The other mode results from the translation invariance and induces zig-zag perturbations; it is always stable. Further modes exist but they are all strictly negative for all  $k$ . Dispersion relations for several of the eigenvalues and the associated eigenfunctions  $h_1$  are shown in the top and bottom row of Fig. 10. The results in the left and right columns are for different mobilities, that is,  $h^2$  and  $h^3$ .

An asymptotic analysis for the sharp interface limit  $\epsilon \rightarrow 0$  reveals that to leading order<sup>21</sup>, the dispersion relation of the top eigenvalue only depends on the minimum value of  $\phi(h_*)$  (and hence on the effective contact angle) but not on other details of the potential. To illustrate this point, we include also the dispersion relation using standard the potential (1), see dotted and full lines in Fig. 10.

### 4.2 Beyond linear theory

We now consider nonlinear simulations using the stationary ridge with very small monochromatic perturbations as initial data. Specifically, we consider four choices for  $k$  which satisfy

$$k < k_m, \quad k \approx k_m, \quad k_m < k < k_c, \quad k \approx k_c,$$

and carry out simulations with the mobilities  $h^2$ ,  $h^3$ . The results are shown on the right of Fig. 9.

As long as the perturbations are small enough, the evolution of the corrugations in the nonlinear model closely follow the predictions from the linear stability analysis. Once the perturbations become comparable to the size of the rim ( $\max_x |h - h_0| \approx 1$  for a

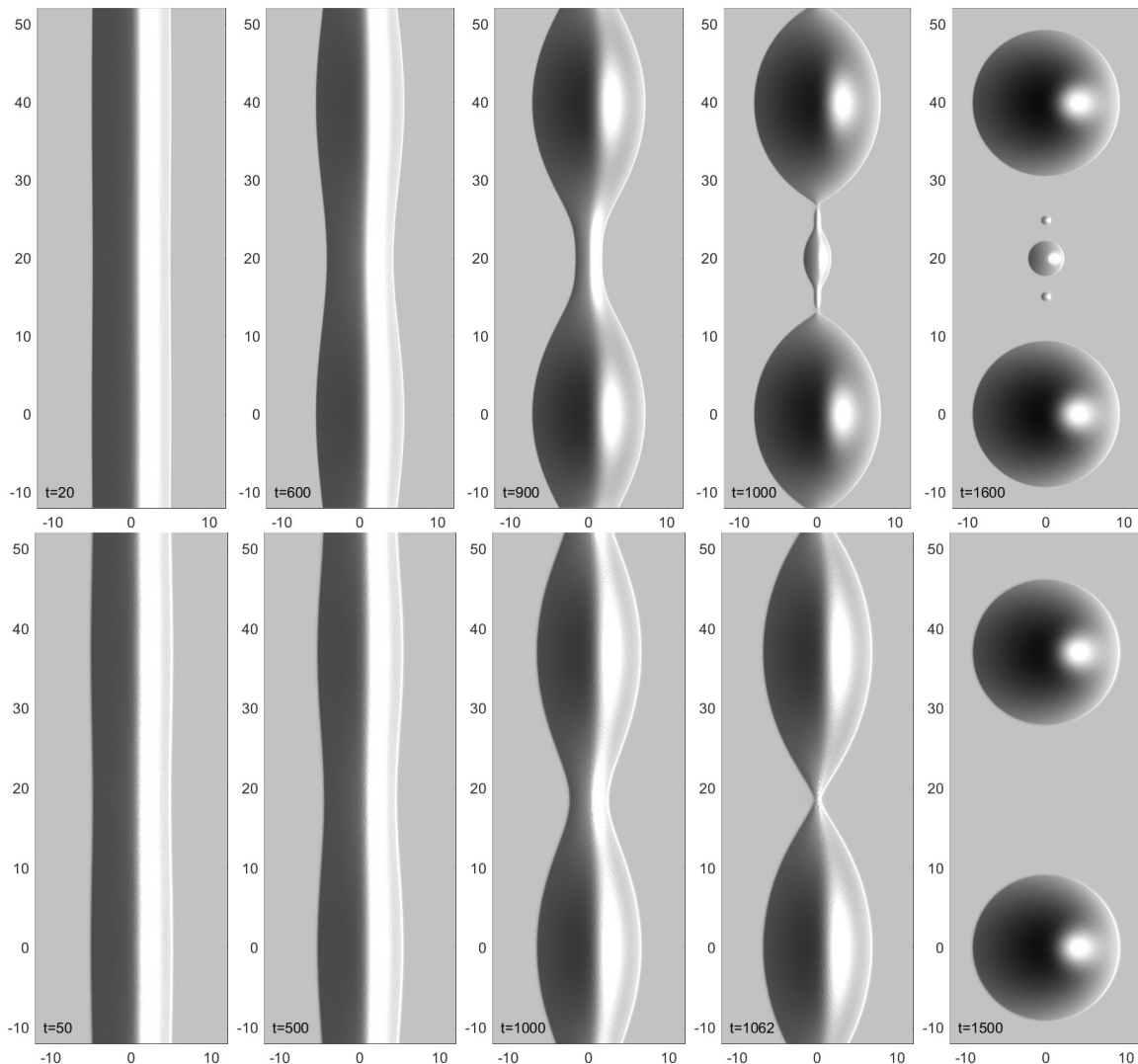


**Fig. 11** Solution of thin-film problem with (**top**)  $m(h) = h^3$  and (**bottom**)  $m(h) = h^2$  and initial data  $h(0, x, y) = h_0(x) + \delta h_1(k; x) \cos(ky)$  at different times. The wavenumber  $k$  is the one with the largest amplification  $\sigma$  from Fig. 10 and the domain  $\Omega = [-12, 0] \times [0, \pi/k]$  is then extended to  $[-12, 12] \times [-\pi/k, 3\pi/k]$  using the implied symmetry of the solution

base state with  $\max_x h_0 = 2.5$ ), nonlinear terms become relevant and the growth rate changes.

Regarding the morphological evolution of the ridges for the no-slip and intermediate-slip case, our numerical simulations show qualitative and quantitative very similar behaviour during the linear regime. However, deep into the nonlinear regime the break-up into droplets follows different scenarios. In the no-slip case a cascade of satellite droplets emerge, while for the intermediate-slip case they disappear. Starting with the same initial condition, the evolution for both cases is shown in Fig. 11. Interestingly, this different behaviour is also observed in our experimental results as seen in Fig. 12.

## 5 Conclusion and discussion

We have introduced a highly adaptive FEM based numerical approach that correctly captures the complex dewetting process described by a class of thin-film models with degenerate mobilities. We showed that for the no-slip condition the droplet

pinch-off is absent during the retraction of the rim, while for the intermediate-slip case self-repeating droplet pinch-off occurs in excellent agreement with experimental results.

The ability to resolve the different length scales for long time scales enables also the prediction of new phenomena, such as the formation of satellite droplets as a function of the mobility. The emergence of satellite droplets is well-known during the break-up of liquid jets and the related problem of liquid filaments. For the latter problem destabilisation is due to the difference in the axial contribution to the capillary pressure between thicker and thinner parts. In this system the pressure is higher in the thinner parts and squeezes the liquid into the bulges, thus increasing the perturbation until the filament breaks up. Apart from the huge literature on experimental studies, the problem has sparked numerous numerical and analytical investigations<sup>28,48,49</sup>. In particular the work by Tjahjadi et al.<sup>27</sup>, where the emergence of satellite droplets was captured numerically, and highly the accurate numerical schemes developed by Kim et al.<sup>50</sup> improved the un-

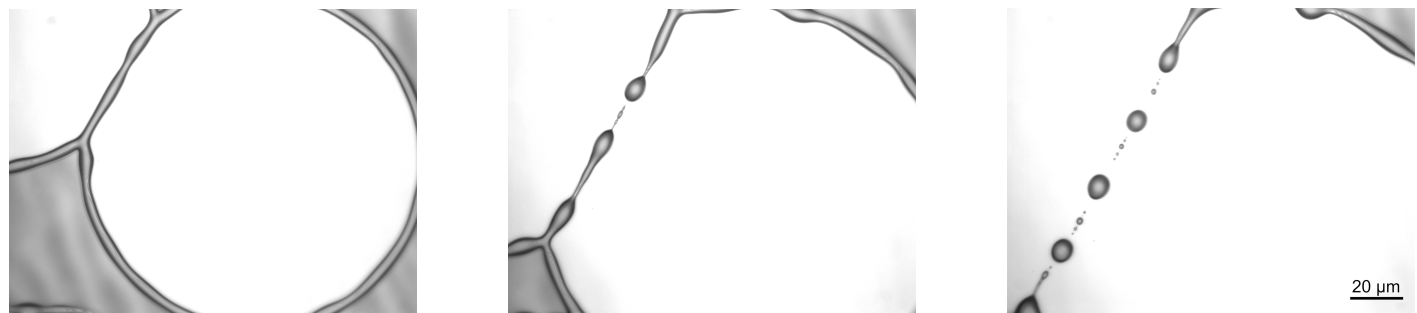


**Fig. 12** Experimental results: Close-up of late stage dewetting of a rim of PS(10.3k) on AF 1600 with time progressing from left to right showing decay into satellite and subsatellite droplets. (Images: Courtesy of L. Marquant<sup>1</sup>)

derstanding the underlying physical processes considerably.

For the situation of a ridge sitting on a solid substrate, considered here, the additional influence of the substrate is present and also enters the linear stability analysis, in particular through the contact angle. It will be interesting to investigate analytically the rupture behaviour for this problem to help understand the influence of the boundary condition at the substrate. Similarly it remains an interesting open question how the dissipation near a moving contact line would affect the whole pattern formation process. Such a study would certainly require more sophisticated finite element techniques<sup>51</sup>.

#### Acknowledgements

We thank Kirstin Kochems for technical assistance. DP acknowledges the financial support of the Einstein Foundation Berlin within the framework of the research center MATHEON.

#### Notes and references

- 1 L. Marquant, *PhD thesis*, 2013.
- 2 E. B. Dussan V., *Annual Review of Fluid Mechanics*, 1979, **11**, 371–400.
- 3 P. G. de Gennes, *Reviews of Modern Physics*, 1985, **57**, 827–863.
- 4 F. Brochard-Wyart and P. de Gennes, *Langmuir*, 1992, **8**, 3033–3037.
- 5 F. Brochard-Wyart and P. de Gennes, *C. R. Acad. Sci. Ser. II*, 1993, **327**, 13–17.
- 6 F. Brochard-Wyart, P.-G. de Gennes, H. Hervet and C. Redon, *Langmuir*, 1994, **10**, 1566–1572.
- 7 K. B. Migler, H. Hervet and L. Léger, *Phys. Rev. Lett.*, 1993, **70**, 287–290.
- 8 L. Léger, *J. Phys.: Condensed Matter*, 2003, **15**, S19–S29.
- 9 E. Lauga, M.P.Brenner and H. Stone, *Handbook of Experimental Fluid Dynamics*, Springer, New York, 2007, pp. 1219–1240.
- 10 L. Bocquet and J. L. Barrat, *Soft Matter*, 2007, **3**, 685–693.
- 11 C. Redon, F. Brochard-Wyart and F. Rondelez, *Phys. Rev. Lett.*, 1991, **66**, 715–718.
- 12 C. Redon, J. B. Brzoska and F. Brochard-Wyart, *Macromolecules*, 1994, **27**, 468–471.
- 13 G. Reiter and R. Khanna, *Langmuir*, 2000, **16**, 6351–6357.
- 14 K. Jacobs, R. Seemann, G. Schatz and S. Herminghaus, *Langmuir*, 1998, **14**, 4961–4963.
- 15 P. Damman, N. Baudelet and G. Reiter, *Phys. Rev. Lett.*, 2003, **91**, 216101.
- 16 R. Fetzer and K. Jacobs, *Langmuir*, 2007, **23**, 11617–11622.
- 17 J.-L. Masson, O. Olufokunbi and P. F. Green, *Macromolecules*, 2002, **35**, 6992–6996.
- 18 F. Brochard-Wyart and C. Redon, *Langmuir*, 1992, **8**, 2324–2329.
- 19 G. Reiter and A. Sharma, *Phys. Rev. Lett.*, 2001, **80**, 166103.
- 20 S. Haefner, M. Benzaquen, O. Bäumchen, T. Salez, R. Peters, J. D. McGraw, K. Jacobs, E. Raphaël and K. Dalnoki-Veress, *Nature communications*, 2015, **6**, 7409.
- 21 J. King, A. Münch and B. Wagner, *Nonlinearity*, 2006, **19**, 2813–2831.
- 22 A. Münch, B. Wagner and T. P. Witelski, *J. Engr. Math.*, 2006, **53**, 359–383.
- 23 K. Kargupta, A. Sharma and R. Khanna, *Langmuir*, 2004, **20**, 244–253.
- 24 S. H. Davis, *Journal of Fluid Mechanics*, 1980, **98**, 225–242.
- 25 K. Sekimoto, R. Oguma and K. Kawasaki, *Annals of Physics*, 1987, **176**, 359–392.
- 26 J. A. Diez, A. G. González and L. Kondic, *Physics of Fluids*, 2009, **21**, 082105.
- 27 M. Tjahjadi, H. A. Stone and J. M. Ottino, *Journal of Fluid Mechanics*, 1992, **243**, 297–317.
- 28 J. Eggers and E. Villermaux, *Reports on Progress in Physics*, 2008, **71**, 036601.
- 29 R. Seemann, S. Herminghaus and K. Jacobs, *Physical Review Letters*, 2001, **86**, 5534.
- 30 R. Seemann, S. Herminghaus and K. Jacobs, *Journal of Physics: Condensed Matter*, 2001, **13**, 4925.
- 31 O. Bäumchen, L. Marquant, R. Blossey, A. Münch, B. Wagner and K. Jacobs, *Phys. Rev. Lett.*, 2014, **113**, 014501.
- 32 P. L. Evans, J. R. King and A. Münch, *Applied Mathematics Research eXpress*, 2006, **2006**, 1–25.
- 33 R. Fetzer, K. Jacobs, A. Münch, B. Wagner and T. P. Witelski, *Phys. Rev. Lett.*, 2005, **95**, 127801.
- 34 R. Fetzer, A. Münch, B. Wagner, M. Rauscher and K. Jacobs, *Langmuir*, 2007, **23**, 10559–10566.

- 35 R. Fetzer, M. Rauscher, A. Münch, B. A. Wagner and K. Jacobs, *Europhysics Letters (EPL)*, 2006, **75**, 638–644.
- 36 O. Bäumchen, R. Fetzer and K. Jacobs, *Phys. Rev. Lett.*, 2009, **103**, 247801.
- 37 O. Bäumchen and K. Jacobs, *J. Phys. Condens. Matter*, 2010, **22**, 033102.
- 38 J. C. Flitton and J. R. King, *J. Engr. Math.*, 2005, **50**, 241–266.
- 39 J. D. McGraw, O. Bäumchen, M. Klos, S. Haefner, M. Lessel, S. Backes and K. Jacobs, *Advances in colloid and interface science*, 2014, **210**, 13–20.
- 40 A. Münch and B. Wagner, *Physica D*, 2005, **209**, 178–190.
- 41 M. Dziwnik, M. Korzec, A. Münch and B. Wagner, *Multiscale Modeling & Simulation*, 2014, **12**, 755–780.
- 42 J. King, A. Münch and B. Wagner, *J. Engrg. Math.*, 2009, **63**, 177–195.
- 43 O. Lessel, O. Bäumchen, M. Klos, H. Hähl, R. Fetzer, M. Paulus, R. Seemann, and K. Jacobs, *Surf Interface Anal.*, 2015, **47**, 557.
- 44 O. Bäumchen, R. Fetzer, M. Klos, O. Lessel, L. Marquant, H. Hähl and K. Jacobs, *J. Phys.:Condens. Matter*, 2012, **24**, 325102.
- 45 O. Bäumchen, R. Fetzer, A. Münch, B. Wagner and K. Jacobs, *IUTAM Symposium on advances in micro- and nanofluidics*, 2009, 0 ISBN: ISBN 2–906831–76–X.
- 46 L. Zhornitskaya and A. L. Bertozzi, *SIAM Journal on Numerical Analysis*, 1999, **37**, 523–555.
- 47 G. Grün and M. Rumpf, *Numerische Mathematik*, 2000, **87**, 113–152.
- 48 J. Eggers, *Rev. Mod. Phys.*, 1997, **69**, 865–930.
- 49 A. L. Bertozzi, *ZAMM - Journal of Applied Mathematics and Mechanics / Zeitschrift für Angewandte Mathematik und Mechanik*, 1996, **76**, 373–419.
- 50 J. Kim, K. Kang and J. Lowengrub, *Journal of Computational Physics*, 2004, **193**, 511 – 543.
- 51 D. Peschka, *Physics of Fluids*, 2018, **30**, 082115.